Molecular Therapy
Original Article

FLT201, a novel liver-directed AAV gene therapy candidate for Gaucher disease type 1

Fabrizio Comper,[1,7] Carlos J. Miranda,[1,7] Benjamin Liou,[2] Tihomir Dodev,[1] Jey M. Jeyakumar,[1] Miriam Canavese,[1] Clement Cocita,[1] Khashayar Khoshrou,[1] Gustavo Tiscornia,[3] Elisa Chisari,[1] Emmaline Stotter,[1] Erald Shehu,[1] Sudharsan Sridharan,[1] I-Mei Yu,[1] Jalpa Pandya,[1] Jaminder Khinder,[1] Natalie Northcott,[1] Petya Kalcheva,[1] Samantha Correia,[1] Ying Sun,[2,5] Allison P. Dane,[1] Rose Sheridan,[1] Amit C. Nathwani,[4,6] and Romuald Corbau[1]

[1]Spur Therapeutics, Stevenage SG1 2BP, UK; [2]Division of Human Genetics, Cincinnati Children's Hospital Medical Center, Cincinnati, OH 45229, USA; [3]Center for Marine Sciences, University of Algarve, 8005-139 Faro, Portugal; [4]Katharine Dormandy Haemophilia and Thrombosis Centre, Royal Free Hospital, London NW3 2QG, UK; [5]Department of Pediatrics, University of Cincinnati College of Medicine, Cincinnati, OH 45229, USA; [6]University College London Cancer Institute, London WC1E 6DD, UK

Gaucher disease type 1 (GD1) is caused by mutations in the *GBA1* gene, which result in deficient enzyme β-glucocerebrosidase (GCase) activity and production with the harmful accumulation of the lipid substrate glucocerebroside. Replacement of GCase is current standard of care for GD1; however, GCase has a relatively short active half-life at both physiological and lysosomal pH and biweekly intravenous administration does not provide a consistent exposure to active enzyme. FLT201 is the first adeno-associated virus (AAV) gene therapy in clinical trials for treatment of GD1. FLT201 consists of a rationally designed AAV capsid (AAVS3) containing an expression cassette with an engineered *GBA1* transgene that encodes a unique glucocerebrosidase variant (GCase85). GCase85 includes an engineered disulfide, which results in a >6-fold increase in active half-life in human serum and a >21-fold increase in active half-life at lysosomal pH conditions, with similar catalytic properties to those of wild-type and exogenous GCase. Preclinical data indicate that FLT201 could offer a durable treatment for Gaucher disease type 1, addressing unmet needs related to substrate accumulation in tissues poorly treated by current enzyme replacement therapy. The improved stability of the engineered GCase85 variant is predicted to be crucial for FLT201's therapeutic effectiveness.

INTRODUCTION

Gaucher disease is a rare autosomal recessive genetic disease caused by mutations in the *GBA1* gene, which encodes the enzyme β-glucocerebrosidase (GCase).[1] GCase deficiency leads to accumulation of the lipid substrates glucocerebroside and the clinical biomarker glucosylsphingosine (lyso-Gb1); macrophages become engorged with these lipid substrates, forming what are known as Gaucher cells, which aggregate in organs and tissues to cause organ inflammation and dysfunction.[1,2]

Gaucher disease type 1 is the most common form of the disease in most Western countries, accounting for over 90% of all cases in Europe and the United States,[1] and has a prevalence of ∼0.70–1.75 per 100,000 births.[2] In contrast to other forms of Gaucher disease, type 1 disease is characterized by the accumulation of Gaucher cells in multiple organs, including the spleen, liver, and bone marrow, but not in the central nervous system.[1,2] The nature and severity of the symptoms of Gaucher disease type 1 vary widely between individuals, but common presentations include hepatosplenomegaly, bone pain and fractures, anemia and fatigue, and thrombocytopenia causing bleeding and bruising.[1–3]

The current standard of care for patients with Gaucher disease type 1 is enzyme replacement therapy (ERT), which involves intravenous delivery of functional wild-type (WT) GCase enzyme at regular intervals (∼2 weeks).[4,5] An alternative to ERT is substrate reduction therapy (SRT), an oral treatment that aims to decrease glucocerebroside production, but is only suitable for some patients.[1,5–7] Although the introduction of ERT and SRT has led to a dramatic improvement in outcomes, responses can be variable and incomplete[8,9]; as a result, some patients continue to experience substantial life-limiting symptoms (e.g., bone disease, lung disease, and an increased risk of hematological malignancies) and a poor quality of life.[5,8–11] In addition, the life-long nature of treatment can be burdensome for patients, and the cumulative health care costs are high.[5,7,10] There remains, therefore, an unmet need for effective therapies.

Gene therapy has the potential to transform treatment of monogenic disorders, e.g., Gaucher disease.[12,13] The goal of gene therapy is to provide a long-lasting treatment that delivers functional *GBA1* to enable the body to produce active GCase, thus offering a functional cure.[12,13]

Received 10 December 2024; accepted 2 May 2025;
https://doi.org/10.1016/j.ymthe.2025.05.003.

[7]These authors contributed equally

Correspondence: Rose Sheridan, Sycamore House, Gunnels Wood Road, Stevenage SG1 2BP, UK.
E-mail: rose.sheridan@spurtherapeutics.com

Early attempts to administer unmodified GCase failed to consistently deliver clinically meaningful benefits due to the short half-life and predominant hepatic uptake of unmodified GCase.[14] Importantly, a key feature in the development of functional ERTs has been the effort spent on securing a GCase glycosylation profile targeting macrophages via the CD206 receptor and, hence, to the spleen as well as the liver, which are the main organs showing pathological changes in Gaucher disease.[1,2] However, while the glycosylation profile has been optimized between wild-type GCase (GCase-WT) and different ERTs, the enzymatic activity, stability, in-cell stability, and murine *in vivo* distribution and function remain similar.[15,16]

Unlike glycosylation-modified recombinant enzymes, for a liver-directed gene therapy the expressed transgene protein is wholly dependent on the target cell machinery for complex, structurally diverse glycosylation. Other than altering GCase at an amino acid level to change *O*- or *N*-linked sites of glycosylation, there is limited scope to influence the glycosylation profile of the expressed enzyme. We needed, therefore, to explore alternative ways to secure the appropriate GCase exposure required to reduce or eliminate substrate accumulation. In this context, our attention turned to providing sufficient stability/half-life of GCase in circulation to ensure plasma levels supporting the ability of GCase to reach cells and tissues beyond the macrophages that are less accessible to ERT (e.g., lung). More importantly we sought to significantly increase the lysosomal stability of GCase to enable sustained catalytic action where it is needed to act on its substrates. With this in mind, we aimed at a mode of action that bridges ERT and SRT. GCase delivered via gene therapy is designed to break down substrates during the initial accumulation across the body, rather than acting only after uptake by macrophages.

To achieve this goal, a panel of rationally designed GCase variants was evaluated leading to the identification of the unique variant GCase85, which has substantially improved structural stability due to the introduction of a disulfide bridge. Herein, we describe the design of the clinical candidate FLT201, which utilizes the rationally designed liver tropic adeno-associated virus S3 (AAVS3)[17] capsid to deliver a codon-optimized *GBA1* transgene encoding GCase85 under a strong,[18] clinically validated,[19] liver-specific promoter comprising the human apolipoprotein E/C-I gene locus control region (HCR)[20,21] and the human α1-anti-trypsin (hAAT) promoter.[22] Additionally, the tissue coverage and efficacy of this novel construct is investigated in preclinical studies supporting FLT201 gene therapy to deliver a long-lasting and effective treatment for Gaucher disease type 1, addressing challenges such as substrate buildup in organs that remain untreatable by current therapies. FLT201 is currently being investigated in a first-in-human, phase 1/2 clinical trial for the treatment of Gaucher disease type 1 (GALILEO-1; NCT05324943).[23]

RESULTS

In vitro identification of GCase variants with improved stability compared with GCase-WT

To improve the structural stability of GCase, we designed 86 variants and expressed them in mammalian cells (Expi293) to assess their *in vitro* stability. In an initial screen, after incubation at neutral pH for 2 h in phosphate-buffered saline, 10 of the GCase variants showed improved stability compared with the GCase-WT protein (Figure 1A). Variants GCase-21 and GCase85 retained the highest levels of GCase activity. GCase-21 incorporates a single amino acid substitution, E272Q; GCase85 incorporates two amino acid substitutions, W351C and A380C, which result in a putative novel disulfide bond in the protein structure, contributing to the observed increase in stability of the variant relative to the WT protein (residue numbering refers to NCBI Reference Sequence: NP_000148.2 for WT protein; computer-modeled structure of GCase85 in Figure S1). Hit confirmation of GCase-21, GCase85, and GCase-21/85 (a protein combining the E272Q, W351C, and A380C mutations) found the hits retained significant activity relative to GCase-WT over 7 days at neutral (Figure 1B) and acidic pH (Figure 1C).

The activity and stability of the products of the transgenes *GBA1-21*, *GBA1-85,* and *GBA1-21/85,* expressed from identical base vectors with the same sequence optimization, were assessed following secretion in Huh7 serum-free growth media after AAVS3 transduction using a 15-point, 2-fold serial dilution of multiplicity of infection (MOI) starting at 1×10^6 vector genome [vg]/cell. GCase85 showed up to 100-fold higher activity levels than GCase-WT (Figure 1D). Similarly, AAVS3-mediated expression of *GBA1-85* resulted in higher GCase activity levels than either *GBA1-21* or *GBA1-21/85*. As a liver-directed gene therapy, functional transduction of liver cells is as important as expressed protein properties. This functional transduction was reflected in the GCase85 vector potency for expression in an Huh7 cell line (EC50) with a 2.8-fold increase in potency compared with GCase-WT (Figure 1E).

Based on initial screening, GCase85 was identified as a lead and the biophysical properties of this variant relative to velaglucerase alfa (VPRIV, Takeda Pharmaceuticals)[24] were examined further. When tested at lysosomal and physiological pH as well as in multiple media including mouse, primate, human serum and/or plasma, GCase85 consistently showed improved stability relative to recombinant GCase-WT (velaglucerase alfa). GCase85 had a 1.7-fold to >26-fold longer active half-life, with a 3°C increase in thermostability at both pH 7 and pH 5.75 and without a significant difference in catalytic properties (Table S1). Although GCase85 does show a 2-fold increase in k_{cat}, this is considered to be at least partly due to the poor stability of recombinant GCase-WT compared to GCase85 in this analysis.

In silico assessment of potential immunogenicity risk profiles of GCase-WT and GCase85

In silico analysis was used to investigate the potential immunogenicity risk profile of GCase-WT and GCase85. For human leukocyte antigen (HLA) class I and II receptors, GCase-WT and GCase85 had similar numbers of strong and intermediate binders (Table 1). For HLA class I, GCase-WT had 19 strong and 36 intermediate binders, while GCase85 had 16 strong and 38 intermediate binders (Table 1; Figure 2A). For HLA class II, GCase-WT had 36 strong and 100 intermediate binders, while GCase85 had 32 strong and

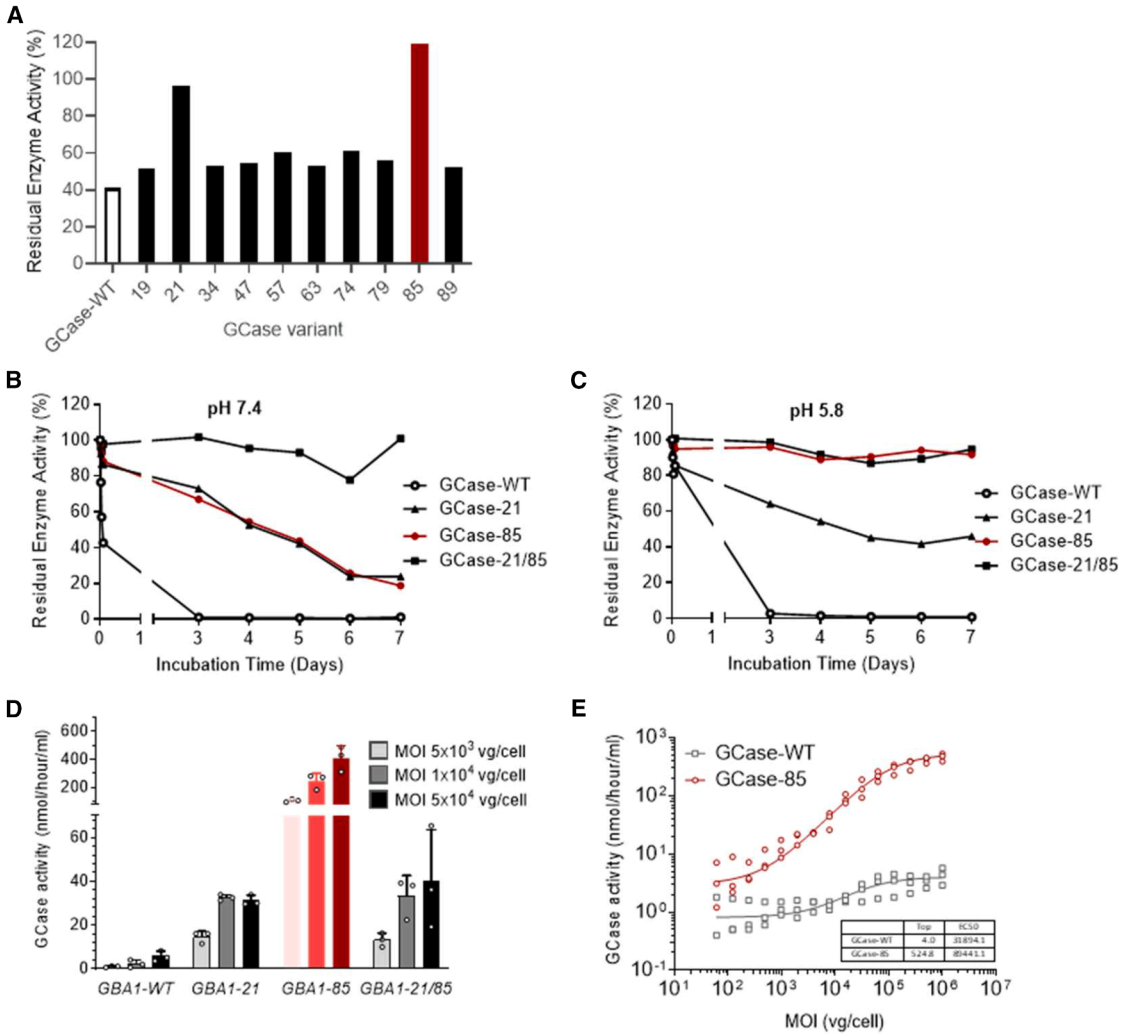

Figure 1. GCase85 shows increased stability compared with GCase-WT

(A) Relative stability of GCase-WT (white) and GCase variants (black and red; equal volumes of conditioned media were tested) after 2 h of incubation at neutral pH (in PBS) (N = 1 for GCase-WT and each variant). (B and C) Residual enzyme activity observed with GCase-WT and the top three lead GCase variants when incubated at 37°C for 7 days at pH 7.4 (serum-free growth medium) (B) or pH 5.6 (C) (N = 1 for GCase-WT and each variant). (D) Levels of GCase activity observed in Huh7 cell culture supernatant at 3 days post-transduction with AAVS3 encoding either *GBA1-WT* or *GBA1* variants. Data are mean (SD) of triplicate wells. Untreated samples were also assessed, and all measures were below the limit of detection (data not plotted). (E) Vector dose-response of GCase85 and GCase-WT secreted from Huh7 cells at 3 days after transduction with AAVS3-*GBA1-85* (FLT201) and AAVS3-*GBA1-WT*, respectively. Data are mean (SEM) of three independent experiments. GCase enzyme activity was determined fluorometrically. AAV, adeno-associated virus; GCase, glucocerebrosidase; MOI, multiplicity of infection; PBS, phosphate-buffered saline; SD, standard deviation; SEM, standard error of the mean; vg, vector genome; WT, wild type.

99 intermediate binders (Table 1; Figure 2B). Importantly, no new peptide binders were identified and overall, this suggests that GCase85 has similar immunogenicity risk to GCase-WT.

Uptake of GCase85 in human cells

To assess whether GCase85 encoded by FLT201 can be taken up by Gaucher disease-relevant cells of human origin, multiple cell types including peripheral blood mononuclear cells (PBMCs), THP-1-derived macrophages, Gaucher disease patient-derived fibroblasts, and Gaucher disease induced pluripotent stem cell (iPSC)-derived macrophages were incubated with either purified GCase85 or cell culture supernatant collected from FLT201-transduced Huh7 cells. ERT (velaglucerase alfa) was tested in parallel.

Concomitant dose-dependent uptake and elevated levels of GCase enzyme activity were detected in PBMCs, THP-1-derived macrophages, and Gaucher disease patient-derived fibroblasts following exposure to GCase85 or ERT. Overall, the data suggest concentration-dependent biphasic uptake kinetics, with greater relative uptake at ≥0.5 μg/mL (Figures 3A–3C). At an exogenous concentration of

Table 1. Peptide binding categorization

HLA class	Peptide binding category[a]	GCaseWT	GCase85
HLA I	strong	19	16
	intermediate	36	38
HLA II	strong	36	32
	intermediate	100	99

[a]For "strong" binders the calculated IC50 cutoff range used was 0 to ≤50 nM and for "intermediate" binders, >50 to ≤500 nM (http://tools.iedb.org/mhcii/help/).

<1 μg/mL, the uptake in GCase activity was less pronounced in PBMCs than in macrophages derived from THP-1 cells (Figures 3A and 3B). This difference likely reflects the nature of the mixed cell population of PBMCs, which includes up to 10% monocytes that as immature cells do not express significant levels of CD206.[25,26] While similar GCase uptake was observed in THP-1-derived macrophages, at doses 0.1–1 μg/mL, slightly better uptake was observed for ERT. At doses >5 μg/mL, the impact of the improved stability of GCase85 resulting in higher intracellular levels is demonstrated (Figure 3B).

A comparative uptake study was also performed using patient-derived Gaucher disease (types 1 and 2) skin fibroblast cells to compare the uptake efficiency of GCase85 and ERT. Upon GCase exposure, there is clear evidence of uptake in both Gaucher disease type 1 and 2 cell lines at 0.5–5 μg/mL (Figure 3C). However, GCase activity following overnight incubation clearly suggests that GCase85 has greater intracellular stability over ERT and shows noticeable uptake of the enzyme at the lower assessed dose of 0.1 μg/mL (Table S2). Similarly, iPSC-derived Gaucher disease macrophages bearing the mutation L444P demonstrated dose-dependent uptake of GCase85 following 3-h incubation with cell culture supernatant collected from Huh7 cells transduced with increasing MOI of FLT201 vectors (10^4, 10^5, 10^6 vg/cell; Figure 3D).

The glyco-engineered GCase delivered as ERT mainly relies on uptake via CD206-mediated endocytosis into the macrophages.[27] To evaluate if this pathway is also employed for GCase85, the contribution of CD206 in GCase85 uptake in Gaucher disease iPSC-derived macrophages was investigated by adding mannan, which is a well-described CD206 receptor binding ligand that has been shown to partially block GCase uptake *in vitro*.[27,28] In the presence of mannan, a significant decrease in GCase uptake was observed in iPSC-derived macrophages for both GCase85 and ERT (Figure 3E), hence demonstrating that a high-mannose form of GCase85 is produced from both HEK293 and HUH-7 cells. This is consistent with previously published data[27,28] and demonstrates that a substantial fraction of both GCase85 and ERT uptake is mediated by CD206-dependent mechanisms.

Characterization of AAV8-*GBA1-WT* and AAV8-*GBA1-85* in WT mice

AAVS3 was developed for improved human hepatocyte transduction, consists of a viral protein (VP)1u portion from AAV8 with the remainder (i.e., VP2u and VP3) from AAV3B[17] and is the capsid used in two other phase 1/2 liver-directed gene therapy clinical trials for hemophilia B (FLT180a)[17] and Fabry disease (FLT190).[29] Compared with other clinically validated capsids, AAV8, AAV5, and AAVrh10, AAVS3 demonstrated significantly higher hepatic transduction in HUH7 and HepG2 cell lines, primary human hepatocytes, and primary rhesus macaque hepatocytes (Figure S2). Transduction of the humanized liver mouse model (FRG model) with either AAV8 or AAVS3 demonstrated 24% of engrafted human hepatocytes expressed a GFP reporter gene after AAVS3 injection vs. 4.3% of human cells after AAV8 transduction (Figure S3). Transduction of mouse hepatocytes with AAVS3 is, however, significantly less efficient. For this reason, codon-matched wild-type (*GBA1-WT*) and FLT201 genomes (*GBA1-85*; Figure S4) pseudotyped with a recombinant AAV8 capsid (AAV8-*GBA1-WT* and AAV8-*GBA1-85*) was used for mouse studies. The effects of AAV8-*GBA1-85* on levels of GCase activity in plasma in WT (C57BL/6J) mice were dose dependent and sustained (Figure 4A). Mice exposed to AAV8-*GBA1-85* at a dose of 6×10^{10} vg/kg showed a >10-fold increase in plasma GCase compared with mice that received AAV8-*GBA1-WT* at the same dose (Figure 4B). Treatment with *AAV8-GBA1-85* resulted in approximately 4.4-fold, 2.4-fold, and 7.0-fold greater GCase activity in spleen, lung, and bone marrow, respectively, compared with treatment with AAV8-*GBA1-WT* (Figure 4B).

Immunohistochemical analysis confirmed that a single infusion of AAV8-*GBA1-85* (6×10^{10} vg/kg) resulted in substantial uptake of the GCase85 protein into target organs seen at 28 days post-infection, whereas a single infusion of AAV8-*GBA1-WT* (6×10^{10} vg/kg) resulted in barely detectable levels of GCase-WT protein after 28 days (Figure 4C). Importantly, GCase85 was observed in lung and bone marrow, which are difficult-to-reach organs when using ERT in patients with Gaucher disease. Six weeks after administration of AAV8-*GBA1-85* to WT mice, robust and dose-dependent expression of GCase85 was still detected in the liver (Figure 4D). In addition, after administration of AAV8-*GBA1-85*, GCase85 was secreted from the liver, taken up by macrophages in the spleen and trafficked to lysosomes (Figure S5).

Compared with ERT, uptake of GCase following administration of AAV8-*GBA1-85* (2×10^{11} vg/kg) was enhanced and sustained in spleen, lung, and bone marrow (harvested 42 days post-dose) in WT mice (Figure 4E). ERT resulted in uptake of GCase-WT in spleen, but only limited uptake in bone marrow and lung at 1 h post-dose. The level of GCase-WT detected following ERT was transient, with the majority being cleared from all tissues within 24 h (Figure 4E).

Characterization of AAV8-*GBA1-85* in GCase-deficient mice

We assessed the potential of AAV8-*GBA1-85* to restore GCase activity and its catalytic function in the degradation of substrates in in the 9V/null murine model of Gaucher disease with a mixed strain background of C57BL/6, 129SvEvBrd, and FVB as wild-type controls. In these 9V/null mice, a single injection of AAV8-*GBA1-85* resulted

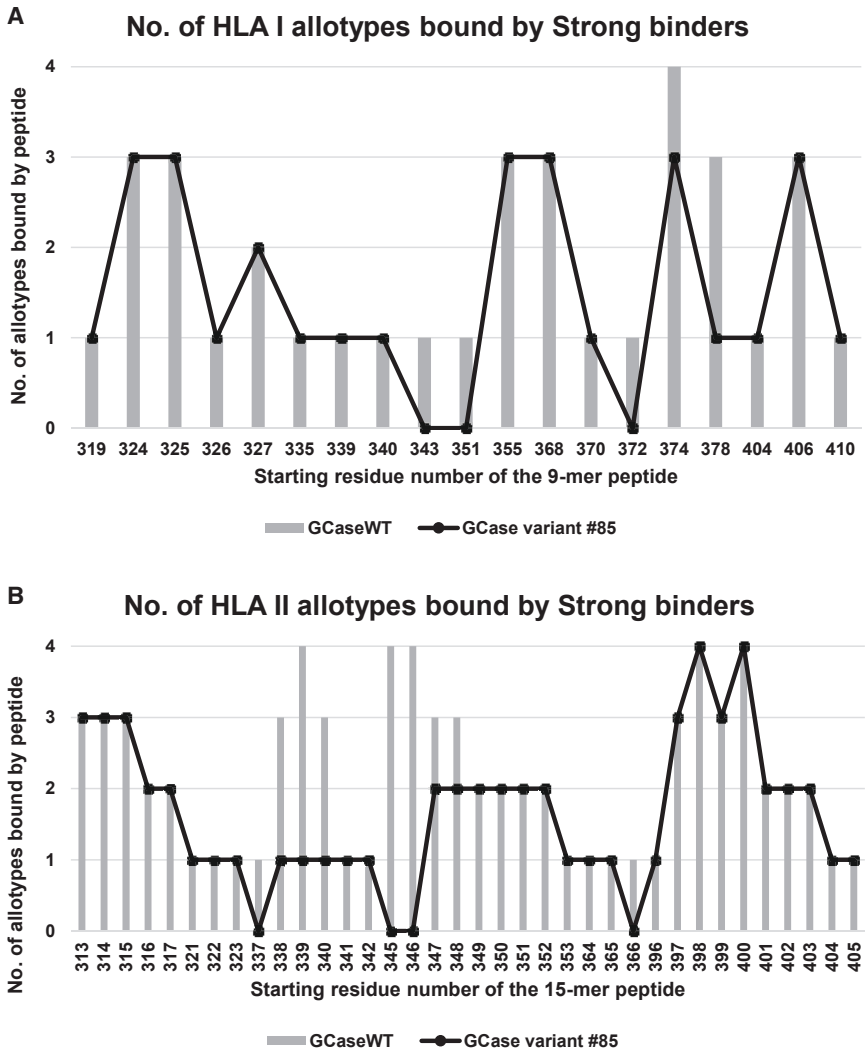

Figure 2. HLA I and HLA II allotype counts for strong binders

The total number of HLA I allotypes (A), including those from both HLA A and HLA B families, bound by the Strong 9-mer binders are shown for GCase-WT (gray bars) and GCase85 (black line). The total number of HLA II allotypes (B), including those from DRB1, DRB3/4/5, DQ and DP families, bound to the Strong 15-mer binders are shown for GCase-WT (gray bars) and GCase85 (black line).

in a dose-dependent increase in GCase activity in the liver, white blood cells (WBCs), bone marrow, spleen, and lung (Figure 5A). No GCase was detected in extracted brain tissue (data not shown). GCase activity following administration of AAV8-*GBA1-85* (2×10^{12} vg/kg) was restored to at least WT levels in all key tissues: spleen (320% of WT levels), lung (132% of WT levels), bone marrow (223% of WT levels), liver (245% of WT levels), and WBCs (121% of WT levels). Following ERT (seven doses, every 2 weeks), GCase activity was restored to near or above WT levels in liver (162% of WT levels), WBCs (94% of WT levels), bone marrow (149% of WT levels), and spleen (191% of WT levels), but not in lung (34% of WT levels; Figure 5A). GCase protein levels tracked well with activity in plasma and across extracted tissues (Table S3). Excluding where there is significant variability at low GCase levels such as ERT in the lung and the low dose of AAV8-*GBA1-85,* or for GBA1-WT in the liver and ERT in the spleen, where poor stability may have impacted the extracted enzyme (Figure S6), the specific activity per ng of GBA1-85 antigen ranged from 0.87–1.39 nmol/h/ng compared with 0.85–0.91 nmol/h/ng for GBA1-WT and 0.77–0.95 nmol/h/ng for ERT. In terms of treatment effect, the specific activity for ERT is significantly lower than that of GBA1-85 ($p \leq 0.001$) in spleen and plasma and lower for GBA1-WT in liver and plasma ($p \leq 0.005$ and $p \leq 0.001$, respectively); however, the variability across tissues would suggest that the impact on specific activity is driven by the improved stability of GBA1-85 compared with GBA1-WT or ERT (Figure S6). In comparison with C57BL/6J wild-type mice (Figure 4A), which have a liver transduction efficiency of near 100% for AAV8, the mouse strain background of the 9V/null mouse model (C57BL/6, 129SvEvBrd, and FVB) (Table S3) gave ~10-fold lower expression from liver-directed gene therapy. The impact of mouse strain background on AAV transduction has been observed for FVB vs. C57BL/6[30] and may account for a proportion of the strain-based differences between the two models.

We evaluated the potential of AAV8-*GBA1-85* to reduce the accumulation of the toxic substrates (glucosylceramide and its breakdown product glucosylsphingosine) in the Gaucher disease mouse model. A single injection of AAV8-*GBA1-85* in 9V/null mice resulted in significant dose-dependent reductions in levels of substrate deposition in plasma and all tissues analyzed compared with untreated mice (glucosylsphingosine: liver, spleen, bone marrow, and lung $p \leq 0.0001$ at 2×10^{11} vg/kg and 2×10^{12} vg/kg, Figure 5B; glucosylceramide: liver and lung $p \leq 0.0001$ at 2×10^{11} vg/kg and 2×10^{12} vg/kg; Figure S7). At a dose of 2×10^{12} vg/kg AAV8-*GBA1-85*, glucosylsphingosine levels in all tissues tested and glucosylceramide levels in plasma, liver, and lung were similar to those observed in WT mice. The impact of AAV8-*GBA1-85* on glucosylceramide accumulation, relative to AAV8-*GBA1-WT*, showed a clear advantage in the lung (and liver) (Figure S7) where there is a higher threshold to achieve normal enzyme levels compared with the macrophage-rich tissues such as the spleen and bone marrow (Figure 5A). Reductions in glucosylsphingosine with ERT treatment

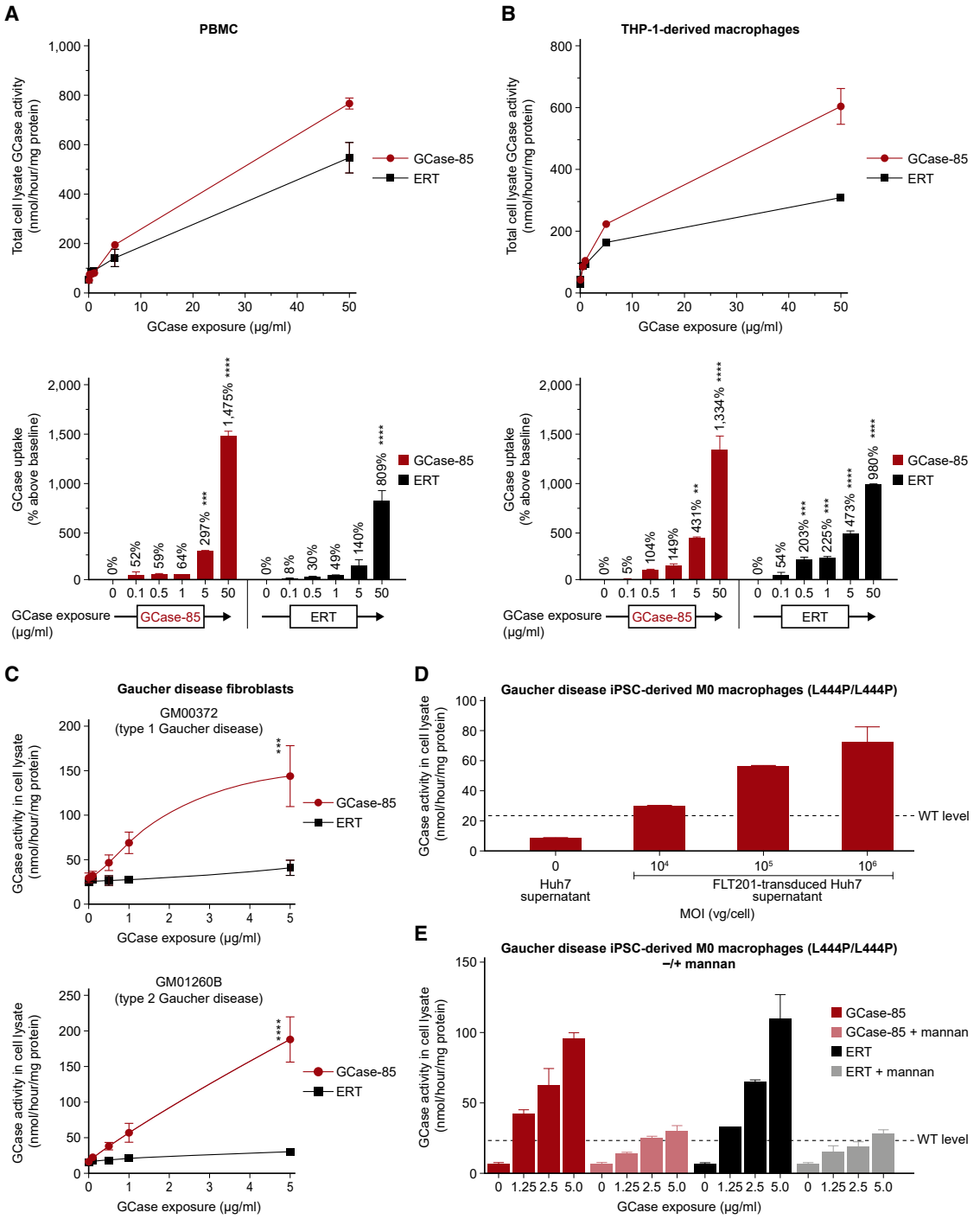

Figure 3. Cellular uptake

The cellular uptake of GCase enzyme was assessed in cultured human cells by exposure of cells to either purified GCase enzyme or supernatant collected from FLT201-transduced Huh7 cells. (A) Uptake analysis in PBMCs following 3-h incubation with purified GCase85 from FLT201 (AAVS3-*GBA1-85*) and commercial recombinant ERT (velaglucerase alfa) at five different concentrations (0.1, 0.5, 1, 5, and 50 µg/mL), expressed as intracellular GCase activity and percentage above the baseline. Data are mean (SD) of duplicate wells and representative of two independent experiments. (B) Uptake analysis in THP-1-derived macrophages following 3-h incubation with purified GCase85 and ERT (velaglucerase alfa) at five different concentrations (0.1, 0.5, 1, 5, and 50 µg/mL), expressed as intracellular GCase activity and percentage above the baseline. Data are mean (SD) of duplicate wells and representative of two independent experiments. (C) Uptake analysis in Gaucher disease patient-derived skin fibroblasts

(legend continued on next page)

were less pronounced than reductions following gene therapy treatments at doses of 2×10^{11} vg/kg and 2×10^{12} vg/kg (Figure 5B). Reductions in glucosylceramide with ERT treatment were less pronounced than reductions following gene therapy treatments at doses of 2×10^{11} vg/kg and 2×10^{12} vg/kg in lung, but equivalent in plasma and liver (Figure S7), again reflecting the observed correction of GCase levels achieved for lung and liver, respectively (Figure 5A).

To evaluate the impact of AAV8-*GBA1-85* on activated macrophages and inflammation, we evaluated the number of storage cells (Figure S8) and CD68 signal density (a marker of inflammation; Figure S9) in 9V/null mice. In the liver of 9V/null mice, treatment with AAV8-*GBA1-85* or ERT significantly reduced the number of storage cells compared with no treatment, with resulting levels similar to those observed in WT mice (Figure 5C). However, in lung, only AAV8-*GBA1-85* treatment resulted in significant reductions in the number of storage cells compared with no treatment ($p \leq 0.0001$). The impact of AAV8-*GBA1-85* was dose dependent; at 2×10^{12} vg/kg, the number of storage cells was similar to that observed in WT mice. In the liver of 9V/null mice, treatment with AAV8-*GBA1-85*, AAV8-*GBA1-WT*, or ERT all resulted in similar reductions in CD68 levels, but in lung the reductions were most pronounced in animals treated with AAV8-*GBA1-85* (Figure 5D).

GCase activity in FLT201-treated nonhuman primates

Seven rhesus macaques were treated with a single infusion of FLT201 (AAVS3-*GBA1-85*) at 2×10^{12} vg/kg and followed for a post-dose observation period of up to 170 days (Figure 6A) or 1,211 days (Figure 6B) (6 or 60 months). All animals were age matched except for animal 7, which was recruited into the study at 1 year old and, as a smaller animal, received ~50% total dose compared with the other animals in the study (Table S4) and reflects difficulty in nonhuman primate (NHP) supply due to the development needs for SARS-CoV-2 vaccines at the time of study. FLT201 treatment resulted in a rapid and robust increase in plasma GCase activity, observed from day 8 and sustained for 170 days (Figure 6A). Fluctuations in GCase levels were noted between day 21 and 43; at day 170, GCase levels ranged from 336 to 1,308 nmol/h/mL plasma, in a similar range to those observed for the 9V/null model at the same dose, pretreatment levels ranged from 7.4 to 9.3 nmol/h/mL. Two animals are still being observed and show stable GCase plasma levels at 1,211 days (3.5 years) ranging from 388 to 1,344 nmol/h/mL (Figure 6B) and will be followed for an additional 1.5 years in an ongoing part of this study. In addition to a lower peak of expression at 559 nmol/h/mL (8 days) compared with the other animals on study (709–2,280 nmol/h/mL at 8 days), a further drop in plasma GCase activity was observed for animal 7 (male) with subsequent recovery and was attributed to transient detectable anti-GCase antibodies that developed in this animal between 154 and 308 days with a total antibody concentration of 1.7–1.8 μg/mL plasma (all other samples were below the limit of quantitation [LoQ] of 32 ng/mL plasma). Additionally, transient detectable anti-GCase antibodies were observed between days 42 and 140 for animal 2 (ranging 2–21 μg/mL plasma) and animal 3 (ranging 2–8 μg/mL plasma). No treatment-related effects on clinical condition, post-dose observations, body weight, food consumption, hematology, blood chemistry, or immunophenotyping of peripheral leukocytes have been observed. Biodistribution of FLT201 is driven by the capsid AAVS3 and has been established for FLT180a at 8 weeks post intravenous (i.v.) dose of 3.41×10^{13} vg/kg (Figure S10). The highest number of vector genome copies (VGCs) were found in the liver and spleen, with geometric mean (range) of 6.02×10^5 VGC/μg DNA (4.05×10^5–9.50×10^5) and 3.3×10^5 VGC/μg DNA (9.2×10^4–1.94×10^6), respectively. Brain, testes, and the dosing site showed the lowest levels of vector genome, with levels in the brain and two out of the three testes evaluated below the lower limit of quantitation (LLOQ 50 copies in 1 μg total nucleic acid). FLT190 showed a similar pattern of distribution at 13 weeks post i.v. dose of 3×10^{13} vg/kg with $n = 3$ males and $n = 3$ females; ovaries showed a geometric mean (range) of 240.07 VGC/μg DNA (73.2–332).

FLT201 was well tolerated in NHPs. Over the 83 days (animal 1), 170 days (animals 2–5), or 1,211 days (animals 6–7) following FLT201 infusion, there were no deaths or treatment-related effects on clinical condition, post-dose observations, body weight, food consumption, hematology, blood chemistry, or immunophenotyping of peripheral leukocytes. Minimal lymphohistiocytic infiltrates observed in the lumbar dorsal root ganglia (DRG) of four FLT201-treated animals were not associated with neuronal degeneration or necrosis, and no lesions were observed in the nerve roots or in the spinal cord. Two FLT201-treated animals had unilateral kidney lymphohistiocytic or lymphoplasmacytic histiocytic infiltrates, which were of mild severity and slightly increased above background levels. The minimal or mild infiltrates in the DRG

following overnight incubation with purified GCase85 and ERT (velaglucerase alfa) at four different concentrations (0.1, 0.5, 1, and 5 μg/mL), expressed as intracellular GCase activity. Data shown as mean (SD) of three independent experiments. (D) Uptake analysis in Gaucher disease iPSC-derived macrophages following 3-h incubation with cell culture supernatant collected from FLT201-transduced Huh7 cells. Data are mean (SD) of two biological replicates. (E) Uptake analysis in Gaucher disease iPSC-derived macrophages following 3-h incubation with purified GCase85 and ERT (velaglucerase alfa) at three different concentrations (1.25, 2.5, and 5 μg/mL), in the presence or absence of mannan (2 mg/mL). Data are mean (SD) of two biological replicates. The WT level (dashed line) in (D) and (E) represents enzyme levels measured in the cell lysates of untreated healthy macrophages derived from a normal iPSC line. $^{**}p \leq 0.01$, $^{***}p \leq 0.001$, $^{****}p \leq 0.0001$ one-way ANOVA with post Tukey correction (multiple comparison test, 95% confidence interval, showing comparison vs. untreated group). Abbreviations: ANOVA, analysis of variance; ERT, enzyme replacement therapy; GCase, glucocerebrosidase; iPSC, induced pluripotent stem cell; MOI, multiplicity of infection; PBMC, peripheral blood mononuclear cells; SD, standard deviation; vg, vector genome; WT, wild type.

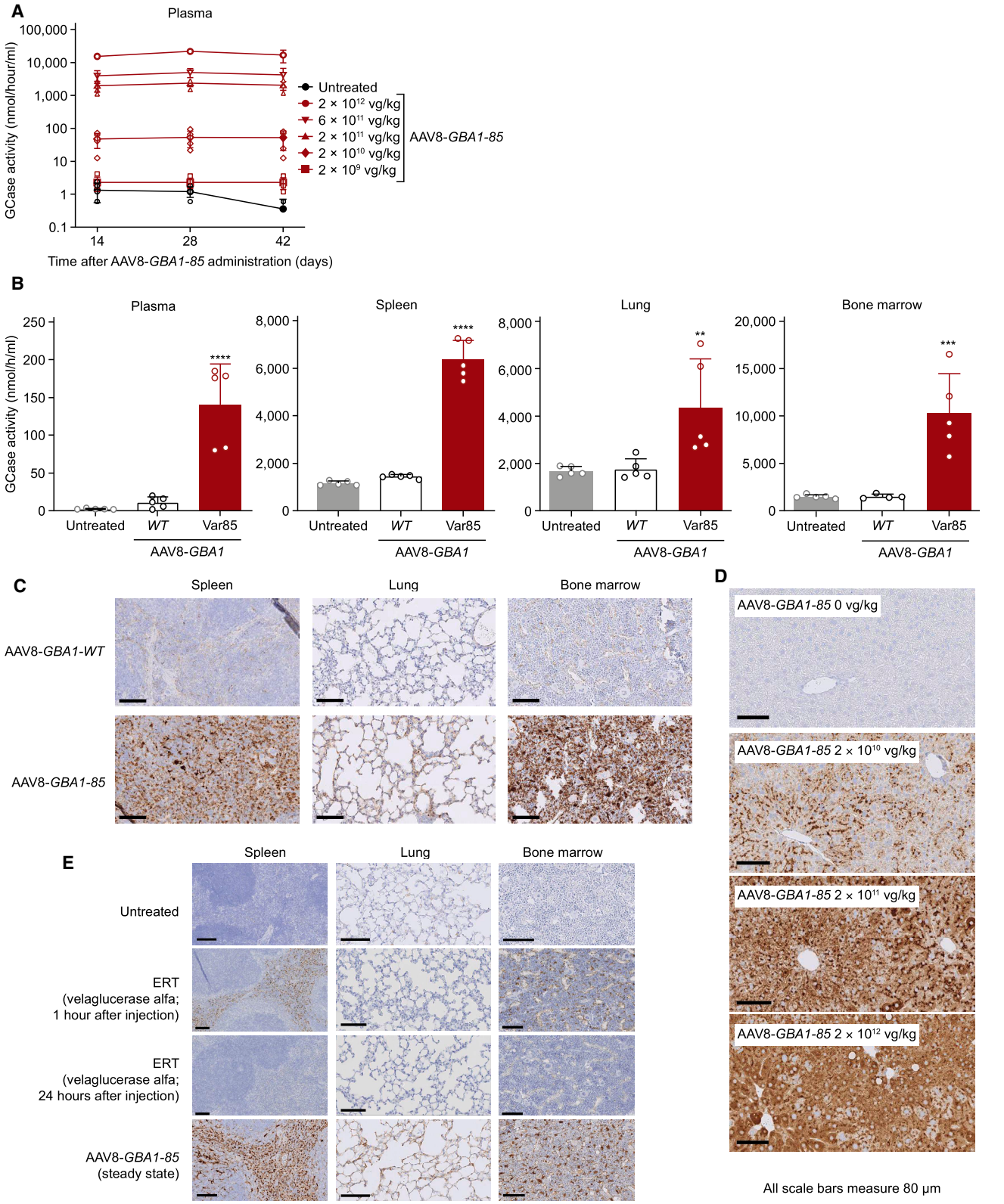

(legend on next page)

and kidneys observed in some FLT201-treated animals were considered not to be adverse and unlikely to be related to the administration of FLT201.

DISCUSSION

Despite providing important improvements in the treatment of patients with Gaucher disease type 1, the effectiveness of ERT, the current standard of care for patients, remains hampered by the relatively short half-life and low stability of GCase-WT.[15,16] Consequently, ERT does not efficiently reach all tissues (e.g., bone and lung[11,15,16,31,32]), to ensure sufficient substrate clearance.[32] In addition, because ERT is administered every 2 weeks, the exposure to active GCase enzyme is not constant,[33] which may allow substrate to accumulate between treatments.[34,35] Substrate accumulation can lead to secondary processes such as inflammation,[36] which are thought to be responsible for unmet medical needs associated with current therapies.[11]

The aim of gene therapy is to provide a consistent supply of endogenous active GCase, which is hypothesized to overcome some of the limitations associated with the intermittent delivery of GCase via ERT.[12,13] Other efforts aimed at developing gene therapy modalities delivering human *GBA1* for Gaucher disease type 1 include the *ex vivo* lentivirus therapy (AVR-RD-02; NCT04145037, NCT04836377) and an AAV9-based gene therapy (LY3884961/PR001, NCT05487599).[37] Both approaches have shown early promise with four out of five patients dosed with AVR-RD-02 experiencing some reduction in spleen and liver size at 52-weeks follow up, and LY3884961 showed an early indication of spleen and liver size reduction in one patient in the 6.8×10^{11} vg/kg low dose cohort.[38] Similar to preclinical data from these two approaches,[39–41] our preclinical data support the hypothesis that administration of *GBA1-WT* via AAV-mediated gene therapy in mice may provide additional benefits vs. ERT in key parameters including tissue exposure, demonstrating advantages of a continuous supply of endogenous enzyme produced in the liver via the *GBA1-WT* gene; however, even with continuous supply of GCase-WT there was a need for further improvement to achieve therapeutic goals.

In agreement with our working hypothesis that enzyme stability is limiting, we demonstrated that administration of gene therapy encoding our disulfide stabilized GCase85 variant produced superior results to both ERT or gene therapy encoding GCase-WT. When compared with GCase-WT in *in vitro* stability experiments, GCase85 was found to have a 6-fold longer active half-life at physiological pH and a >21-fold longer active half-life at lysosomal pH conditions than GCase-WT, while maintaining similar catalytic properties. The large effect on stability at lysosomal pH is particularly important as it enables the intracellular maintenance of active GCase85 and thus, has the potential to represent a more effective treatment for Gaucher disease type 1 than currently available treatments that utilize GCase-WT even when administered in the same regimen.

When delivered by AAV-mediated gene therapy in mouse models, GCase85 substantially enhanced and sustained activity in target organs than either GCase-WT (delivered via gene therapy) or ERT. Importantly, GCase85 activity was detected in tissues that are hard to reach with ERT, such as bone and lung, which likely reflects the greater stability and potentially enhanced biodistribution and increased tissue exposure of GCase85 compared with GCase-WT. The therapeutic value of GCase85 was further demonstrated to reduce toxic substrate levels and inflammatory markers in all affected tissues in the Gaucher disease mouse model.

In NHPs, administration of FLT201 resulted in a robust and sustained increase in plasma GCase activity levels. Of note, although there was a 10-fold difference in GCase plasma activity between C57BL/6J mice and the 9V/null mouse model on dosing with AAV8 constructs, plasma GCase activity levels in NHP dosed 2×10^{12} vg/kg with FLT201 were similar to the 9V/null mice dosed 2×10^{12} vg/kg with AAV8-*GBA1-85*. This difference in plasma activity levels has also been observed for other AAVS3 products, e.g., FLT190, where NHP activity levels were at least five times greater than those with similar constructs using AAV8.[42–44]

FLT201-treated NHPs exhibited no treatment-related adverse effects in males or females. Despite an immune response and formation of antibodies to a foreign (human) protein in NHP, this response was intermittent, resolved and GCase plasma levels recovered over time. This appears to parallel the response that has been observed in humans with ERT, where the formation of antibodies has been observed in <2% of patients for VPRIV and has not limited therapeutic effect.[45] Since FLT201 is liver directed and GCase is produced in host hepatocytes, glycosylation will be host specific and thus be less likely than an exogenous protein to be recognized as foreign.[46] Additionally, targeting the liver for transgene expression is associated with immune tolerance, partly due to the induction of antigen-specific regulatory T cells.[47,48]

Figure 4. AAV8-*GBA1-85* promotes robust levels of GCase secretion into the blood and uptake into target organs

(A) Dose-dependent GCase activity in plasma of WT mice treated with AAV8-*GBA1-85*. Data are mean (SD) (n = 5 mice per group). Two of the five untreated mice had measures of 0.0 at day 42 (these data points are not visible on the chart). (B) Levels of GCase activity observed in plasma, spleen, lung, and bone marrow and of WT mice (n = 5 mice in each group, with the exception of WT bone marrow [n = 4]) following treatment with either AAV8-*GBA1-WT* or AAV8-*GBA1-85* (6×10^{10} vg/kg). Data are mean (SD). (C) Representative images of GCase immunoreactivity observed in target organs 28 days after treatment with AAV8-*GBA1-WT* or AAV8-*GBA1-85* (6×10^{10} vg/kg). (D) Dose-dependent GCase immunoreactivity in liver of WT mice following treatment with AAV8-*GBA1-85*. (E) Representative images of GCase immunoreactivity observed in spleen, lung, and bone marrow after treatment of WT mice (n = 3) with ERT (velaglucerase alfa 60 U/kg) or AAV8-*GBA1-85* (2×10^{11} vg/kg). GCase immunoreactivity, brown; hematoxylin staining, blue. Error bars across images measure 80 μm; $^{**}p < 0.001$; $^{***}p < 0.0005$; $^{****}p < 0.0001$ vs. untreated, one-way ANOVA. Abbreviations: AAV, adeno-associated virus; ANOVA, analysis of variance; ERT, enzyme replacement therapy; GCase, glucocerebrosidase; vg, vector genome; WT, wild type; SD, standard deviation.

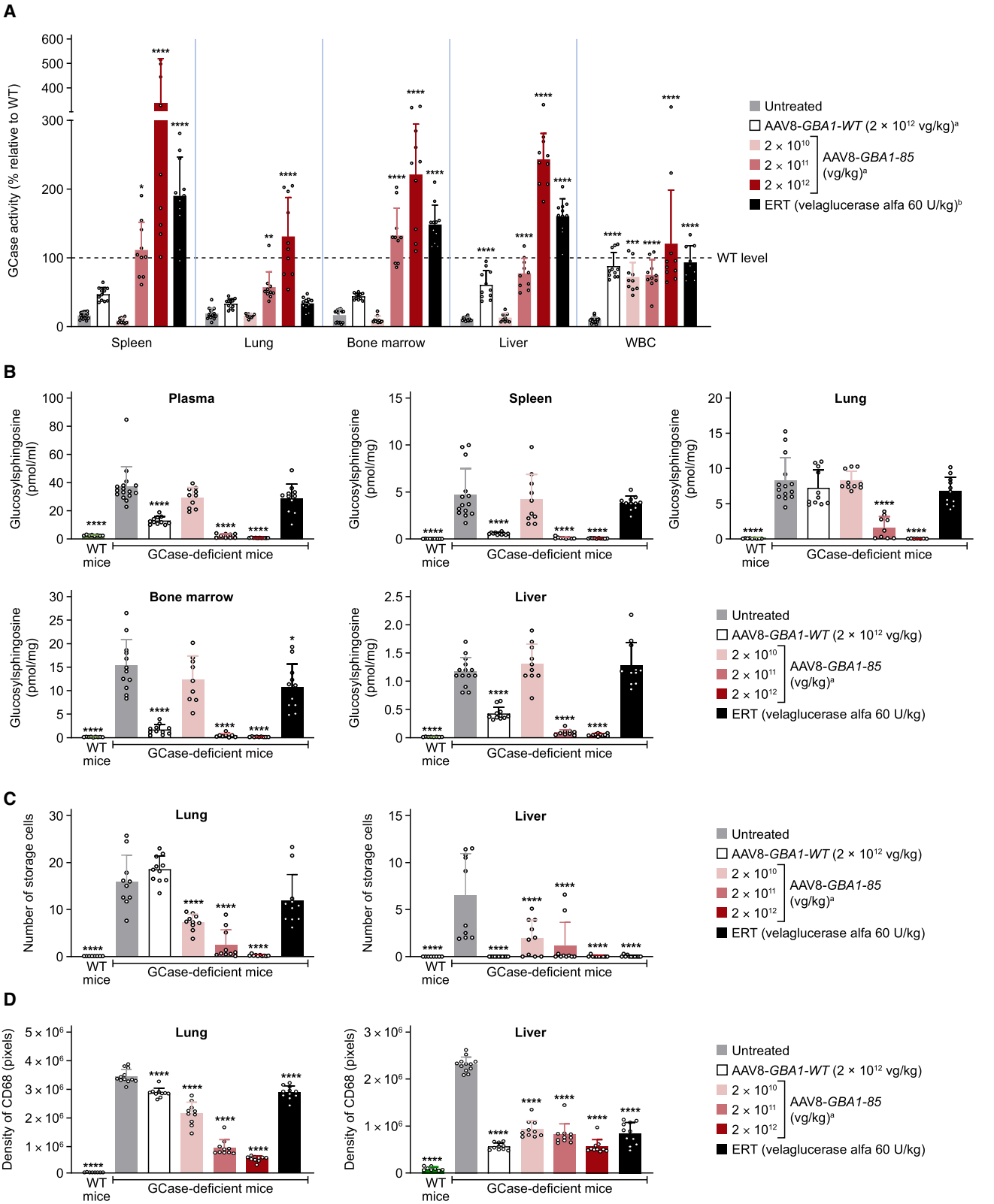

(legend on next page)

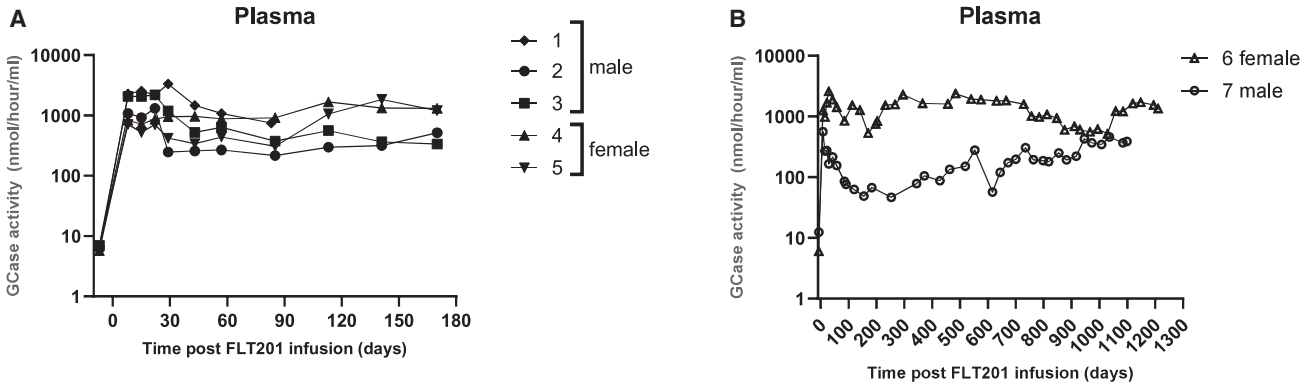

Figure 6. Plasma GCase activity in rhesus macaques following administration of FLT201

(A) Plasma GCase activity after a single intravenous infusion of FLT201 2×10^{12} vg/kg at up to 170 days (6 months). Animal 1 was euthanized at day 83 for early analysis. (B) Plasma GCase activity after a single intravenous infusion of FLT201 (AAVS3-*GBA1-85*) 2×10^{12} vg/kg at up to 1,211 days (3.5 years). Abbreviations: AAV, adeno-associated virus; GCase, glucocerebrosidase; vg, vector genome.

The 9V/null GCase-deficient model established the plasma GCase85 activity levels required to minimize substrate accumulation in key tissues, noting that some tissues such as lung have higher threshold levels for clearance. As a best approximation to humans, the NHP plasma GCase85 activity per FLT201 dosed was utilized to estimate and propose the first-in-human dose of 4.5×10^{11} vg/kg for GALILEO-1 that was anticipated to provide clinical benefit.[23] While AAV9 distributes broadly[49] and LY3884961 may correct tissues locally with ubiquitous expression, we do find that the properties of FLT201 enable effective gene therapy at low viral doses, which may reduce the risk of adverse events and provide an overall beneficial clinical profile. These findings presented here provide preclinical proof-of-concept supporting FLT201 as a potential gene therapy for Gaucher disease type 1 in humans.

The challenge for AAV gene therapy is achieving an acceptable therapeutic window, reliant on potency and dose. While this is being widely addressed through the development of more potent capsids our experience with GCase85 and FLT201 has highlighted that more is required. Hence, we believe that protein engineering will become pivotal in enhancing or altering the pharmacological properties of WT proteins to support their delivery via gene therapy.

Overall, the highly encouraging results from this preclinical study indicate that FLT201 has the potential to provide an effective, long-lasting treatment for Gaucher disease type 1 that could overcome unmet needs associated with the existing standard of care, particularly those related to substrate accumulation in deep tissues. The enhanced stability of the engineered GCase85 variant is anticipated to be a critical factor in driving the efficacy of FLT201 therapy. FLT201 is currently undergoing evaluation in a first-in-human, phase 1/2 clinical trial (GALILEO-1) in adults with Gaucher disease type 1 and shows a favorable safety and tolerability profile with a single low dose of 4.5×10^{11} vg/kg.[50] Clinical parameters and key biomarkers showed sustained improvement or maintenance up to 14 months after withdrawal of ERT or SRT indicating FLT201 has the potential to improve the clinical phenotype of patients with Gaucher disease type 1 by reversing/preventing further lipid substrate accumulation within lysosomes.[50]

MATERIALS AND METHODS

In vitro identification and characterization of β-glucocerebrosidase (GCase) variants

Manufacture of GCase variant proteins

GBA1 variants were generated from nucleotide sequences by gene synthesis and site-directed mutagenesis where appropriate; this was provided together with sequence verification by GenSmart

Figure 5. Impact of AAV8-*GBA1-85* on GCase activity, substrate accumulation and inflammation in visceral tissues in 9V/null mice

(A) GCase activity in 9V/null mice. Data shown as the percentage of GCase activity compared with WT mice in liver, WBCs, bone marrow, spleen, and lung after AAV8-*GBA1-85,* AAV8-*GBA1-WT*, or ERT (velaglucerase alfa) administration (n = 10–11 per group, with the exception of untreated disease control [n = 16] and ERT WBC [n = 9]; spleen and lung from animals dosed 2×10^{11} vg/kg AAV8-*GBA1-85* p = 0.029 and 0.002, respectively). (B) Substrate (glucosylsphingosine) levels in plasma, liver, bone marrow, spleen, and lung of 9V/null mice after AAV8-*GBA1-85*, AAV8-*GBA1-WT*, or ERT (velaglucerase alfa) administration (n = 8–11 per group, n = 16 untreated disease control; bone marrow from animals dosed with ERT (velaglucerase alfa) p = 0.014). (C) Numbers of storage cells in liver and lung of 9V/null mice after AAV8-*GBA1-85,* AAV8-*GBA1-WT* or ERT (velaglucerase alfa) administration (n = 9–11 per group). (D) CD68 signal density in liver and lung of 9V/null mice after AAV8-*GBA1-85,* AAV8-*GBA1-WT* or ERT (velaglucerase alfa) administration (n = 8–12 per group). [a]Data collected 12 weeks after injection. [b]ERT (velaglucerase alfa) was dosed every other week for a total of seven doses. Samples were collected in the 2 h after administration. Values presented correspond to C_{max} expected for tissue uptake on ERT administration. Data represented as mean (SD); $^{*}p \leq 0.05$; $^{**}p \leq 0.01$; $^{***}p \leq 0.001$, $^{****}p \leq 0.0001$ vs. untreated disease control, one-way ANOVA. Abbreviations: AAV, adeno-associated virus; ANOVA, analysis of variance; C_{max}, maximum plasma concentration; ERT, enzyme replacement therapy; GCase, glucocerebrosidase; SD, standard deviation; vg, vector genome; WBC, white blood cell; WT, wild type.

(GenScript, Oxford, UK). DNA sequences were codon optimized (derived from codon usage tables of coagulation factor IX as input to the online application OPTIMIZER[51]) and further manipulated to remove GC motifs, premature stops, and unwanted amino acid substitutions, and to verify cryptic splicing. Codon-optimized nucleotide sequences encoding the GCase variants were cloned into the commercially available expression vector pcDNA5/FRT (Thermo Fisher Scientific, St. Louis, MO).

Transgenes were prepared from nucleotide sequences using the GenSmart gene synthesis platform (GenScript, Oxford, UK) and inserted into plasmid pUC57 (GenScript, Oxford, UK) using standard molecular biology techniques. Plasmid DNA was isolated from *Escherichia coli* and lyophilized until required for use. The identity of each plasmid was confirmed by sequencing prior to use.

Transfection complexes were prepared by adding 80 μL nuclease-free water (Invitrogen, Carlsbad, CA) to 4 μg of lyophilized DNA (*GBA1* variant or wild-type [WT] *GBA1* genes), yielding a final concentration of 50 ng/μL for each construct. The reconstituted DNA (14 μL) was transferred to a 96-well plate and further diluted with 21 μL of Opti-MEM I serum-free medium (plate 1). A working solution of ExpiFectamine (1.9 μL) and Opti-MEM (35 μL) was prepared (plate 2). The contents of the two plates were combined onto a third plate (35 μL from plate 1 and 35 μL from plate 2). After incubation for 20–30 min at room temperature, the DNA-lipid complex was ready to be used for transfection.

To prepare the Expi293F cells (Thermo Fisher Scientific, St Louis, MO) for transfection, they were expanded in suspension in 30 mL of Expi293 medium (Thermo Fisher Scientific, St Louis, MO) at 37°C, 125 rpm, and 8% CO_2 atmosphere, with 80% humidity, in 125-mL plastic flasks with ventilated caps. Cells were split to 0.3×10^6 viable cells/mL when they reached a density of $3–5 \times 10^6$ cells/mL (viability determined using a hemocytometer and trypan blue exclusion).

On the day of transfection, the Expi293F cell concentration was adjusted to a density of 2.8×10^6 cells/mL in individual chambers of a 96-deep-well plate and incubated at 400 rpm at room temperature until the DNA-lipid complex was ready. The DNA-lipid complex (50 μL) was added to the Expi293F cells; the cells were incubated at 37°C in a 5%–8% CO_2 humidified atmosphere at 400 rpm for 16–20 h.

After incubation, a cocktail of Enhancer 1 and Enhancer 2 from the ExpiFectamine 293 transfection kit (27.5 μL/well) (Thermo Fisher Scientific, St Louis, MO) was added. The plate was incubated for a further 4 days (37°C, 5%–8% CO_2 humidified atmosphere, 400 rpm). Plates were centrifuged at $200 \times g$ for 10 min. The supernatant was collected and used in subsequent experiments either without further purification or purified (for further characterization of selected variants) as described in the next paragraph.

Further purification was achieved by clarifying the supernatant by centrifugation at $2{,}000 \times g$ for 30 min. Proteinase inhibitor cocktail tablets (Sigma-Aldrich, Dorset, UK) were subsequently added to the clarified medium according to the manufacturer's instruction. The clarified medium was mixed with *n*-butanol (Sigma-Aldrich, Dorset, UK) at a ratio of four parts medium to one part *n*-butanol (v/v). The solution was mixed (at 4°C for 1–2 h) to allow lipids to partition into the organic fraction, then transferred to a separation funnel. After ≥30 min, the aqueous phase was isolated from the lipid-containing organic fraction. The aqueous phase was loaded at a rate of <1 mL/min to an OctylSepharose CL4B column using the AKTA pure system (Cytiva, Buckinghamshire, UK). The loaded column was washed with two column volumes of each of 25%, 50%, and 75% ethylene glycol (Merck Life Science UK Limited) in 25 mM citric phosphate buffer (Sigma-Aldrich, Dorset, UK) at pH 5.75. GCase proteins were eluted with 75% ethylene glycol in 25 mM citric phosphate buffer, then the buffer was exchanged, using a PD10 column (GE Healthcare, Hatfield, UK), into 25 mM citric phosphate buffer (pH 5.75) and concentrated using Amicon Ultra centrifugal filter (10 kD molecular weight cutoff membrane; Merck, Dorset, UK) to the desired concentration. All batches of GCase-WT or GCase85 used for cellular uptake studies were purified using a two-step process: clarified media was taken to 50 mM NaCHO, 500 mM NaCl, 1 mM MnCl2, 1 mM CaCl2 final concentration. Proteinase inhibitor cocktail tablets (Roche, St Louis, MO) were added according to the manufacturer's instruction and filtered through 0.22 μM. Filtrate was loaded onto a 5 mL HiTrap Con A 4B column (Cytiva, Buckinghamshire, UK) at flow rate 1 mL/min, washed with six column volumes (CV) of binding buffer (25 mM HEPES, 0.5 M NaCl, 1 mM MnCl2, and 1 mM CaCl2). Protein was eluted with 6-CV elution buffer (25 mM HEPES, 0.5 M NaCl, and 1 M methyl α-D glucopyranoside). Fractions containing GCase were pooled and concentrated using a 30,000 molecular weight cutoff spin concentrator and applied to a HiLoad 16/600 Superdex 200 pg size exclusion column (Cytiva, Buckinghamshire, UK), at a flow rate of 0.5 mL/min and eluted with 1.5 CV of elution buffer (25 mM NaCHO, pH ∼5.75), concentrated using a 30,000 molecular weight cutoff spin protein concentrator, filtered through a 0.22 μM membrane pre-equilibrated with the storage buffer (50 mM sodium citrate, pH ∼5.75) and stored at 4°C until use. The average specific activity (SD) of six batches was 11.82 (1.96) 4-MU nmol/h/ng (median = 11.2 4-MU nmol/h/ng) and a representative SDS-PAGE gel of material used in these experiments is presented (Figure S11).

GCase enzyme activity in vitro

GCase enzyme activity was determined fluorometrically using the fluorescent substrate 4-methylumbelliferyl-β-D-glucopyranoside (4-MUG; Sigma-Aldrich, Dorset, UK). Aliquots (20 μL) of the sample were assayed in 100 μL of assay buffer (50 mM sodium citrate [Glentham Life Sciences, Wiltshire, UK], 25 mM sodium taurocholate hydrate, pH 5.75 [Sigma-Aldrich, Dorset, UK]) with 6 mM 4-MUG for 30 min at 37°C. After incubation, 50 μL of stop solution (0.3 M sodium hydroxide [Fisher Scientific], 0.5 M glycine [Glentham Life Sciences, Wiltshire, UK], pH 10) was added. Enzyme activity was

assessed fluorometrically (SpectraMax i3 plate reader [Molecular Devices, Berkshire, UK]; λ_{ex} = 365 nm and λ_{em} = 445 nm). Fluorescence signals were converted to nmol/h/mL based on a 4-methylumbelliferone (4-MU; Sigma-Aldrich, Dorset, UK) standard curve.

For *in vitro* studies, *GBA1-WT* (NCBI Reference Sequence: NP_000148.2) was produced from the pcDNA5/FRT plasmid system and used as a comparator.

GCase in vitro *stability*

The residual activity of each variant was measured after incubation of the unpurified Expi293 cell supernatant in phosphate-buffered saline (PBS) for 2 h.

The variants likely to show improved stability were then assessed in acidic (pH 5.6; AB) or neutral (pH 7.4; PBS) conditions. The purified GCase protein samples were diluted into incubation buffers with an optimal detection range, and enzymatic activity was measured as above such that the initial signal at 0 h was $<1 \times 10^9$ relative fluorescence units (RFU; a response that was neither saturating or near background). The samples were incubated at 37°C without shaking. Aliquots (20 μL) were taken for GCase activity assays after 0, 0.5, 1, and 2 h (in all matrices) and after 3, 4, 5, 6, and 7 days (in serum/plasma only). Stability was measured as percentage of residual activity at each time point.

Production of viral vectors for GBA1 variants and GBA1-WT for characterization in vitro *in Huh7 cells*

The gene encoding human *GBA1* (NCBI Reference Sequence: NM_000157.3) was cloned into an adeno-associated virus (AAV) backbone that drives transgene expression by a liver-specific hepatic control region enhancer/human alpha1 anti-trypsin promoter complex (FRE76). DNA sequences were codon optimized (derived from codon usage tables of coagulation factor IX as input to the online application OPTIMIZER[30]) and further manipulated to remove GC motifs, premature stops, and unwanted amino acid substitutions, and to verify cryptic splicing. This process was repeated for the three *GBA1* variants of interest (*GBA1-21*, *GBA1-85*, and *GBA1-21/85*), such that *GBA1, GBA1-85* (Figure S4), and the other variants all share the same sequence optimization.

Manufacture of viral particles for GBA1 *variants and* GBA1-WT *for* in vitro *and* in vivo *characterization*

Constructs were triple co-transfected into HEK293T cells with plasmids (AAV8 or AAVS3) encoding the AAV Rep and Cap functions, the adenovirus helper functions, and the recombinant genome containing the GCase expression cassette (WT or variant) flanked by AAV2 inverted terminal repeat sequences. AAVS3 vectors were purified with AVB Sepharose affinity chromatography resins (Cytiva, Buckinghamshire, UK). AAV8 vectors were purified with POROS CaptureSelect affinity chromatography resins (Thermo Fisher Scientific, St Louis, MO). Purified stocks were titered by quantitative polymerase chain reaction (qPCR) to the FRE76 promoter region. Single-lot stock titers were as follows: AAVS3-*GBA1-WT* (8.33×10^{11} vg/mL); AAVS3-*GBA1-85* (7.75×10^{11} vg/mL); AAVS3-*GBA1-21* (8.08×10^{11} vg/mL); AAVS3-*GBA1-21/85* (7.86×10^{11} vg/mL); AAV8-*GBA1-WT* (7.33×10^{12} vg/mL); and AAV8-*GBA1-85* (2.7×10^{12} vg/mL).

Manufacture of FLT201 was performed by a contract drug manufacturing organization (CDMO): drug substance used a two-plasmid packaging system[52] and a semi-adherent HEK293T process using iCellis 500 fixed-bed bioreactor (Pall, UK)[53]; drug product titer was 2.21×10^{12} vg/mL, 3.19×10^{13} capsid/mL (by ELISA) and met key quality specifications for endotoxin (<0.05 EU/mL) and bioburden (<1 cfu/10 mL^2).

Activity and stability of GBA1 *variants and* GBA1-WT *in Huh7 cells*

Huh7 cells were maintained in D-10 medium (Dulbecco's Modified Eagle's Medium low glucose [Sigma-Aldrich, Dorset, UK] supplemented with 10% fetal bovine serum [FBS; Gibco, Grand Island, NY] and 1% GlutaMAX [Thermo Fisher Scientific, St Louis, Mo]). For transduction, cells, counted by Countess II FL Automated Cell Counter, were seeded at 2×10^4 cells/well and allowed to adhere for 24 h before transduction. Cells were plated at near confluence to minimize the risk of detachment and to optimize transduction efficiency by reducing opportunities for the vector to contact the cell surface rather than the well wall. Following the 24-h incubation, the transduction mix of D-10, containing the appropriate titer of AAV viral particles for the particular experiment, was prepared and added to the cells (50 μL/well); plates were then incubated overnight at 37°C, 5% CO_2. The following day, the transduction mix was removed by aspiration, and fresh D-10 medium was added to the wells. After 48 h, the medium and cells were collected and analyzed for GCase activity and vector genome (vg) number, respectively. Each transduction was performed in triplicate.

The level of active GCase was determined from the culture supernatant 3 days after transduction (see GCase enzyme activity *in vitro* section above).

Determination of vg number in Huh7 cells

Huh7 cells that had been transduced with *GBA1-85* or *GBA1-WT* were washed with PBS and treated with 40 μL TrypLE (Thermo Fisher Scientific, St Louis, MO) for 5 min. Upon pelleting, PBS 110 μL (Gibco, Grand Island, NY) was added to the cells, which were frozen and stored at −80°C. After three free/thaw cycles to lyse and release DNA, the duplicate wells were pooled and centrifuged (14,000 × *g* for 5 min) before a 15-μL aliquot was taken and diluted (1:33) with nuclease-free water (Life Technologies, Carlsbad, CA).

qPCR was performed on 5-μL aliquots of the diluted cell lysate. Viral genome copy number was determined using primers that bind specifically to the FRE76 promoter sequence (forward: 5′-TTGCTCCT CCGATAACTG-3′; reverse: 5′-GTGCCTGAAGCTGAGGAGAC-3′ [Integrated DNA Technology, Coralville, IA]). Quantitation of

the viral genome was achieved using a dilution curve (1×10^8 vg/reaction to 1×10^3 vg/reaction) using a linearized plasmid.

Each qPCR reaction used 50 ng sample DNA in a total volume of 20 μL of distilled water (forward and reverse primers were used at a working concentration of 500 nM), including 10 μL 2× PowerUp SYBR (Thermo Fisher Scientific, St Louis, MO). Polymerase chain reaction (PCR) was performed using a QuantStudio Real-Time qPCR machine (Thermo Fisher Scientific, St Louis, MO) using the standard cycling mode for primers with a melting temperature of ≥60°C; analysis was performed over a total of 40 cycles. After a PCR run, the validity of the data was checked to confirm that the slope of each standard curve was within 90%–110% of the ideal value of −3.32 (i.e., −3.58 to −3.10), which was indicative a 100% reaction efficiency. An SYBR green melting curve analysis was also included at the end of cycling to confirm the absence of nonspecific duplexes. Data were analyzed with software QuantStudio version 3. The number of viral genomes present in a sample was calculated by reference to the relevant standard curve.

Characterization of biophysical properties of GCase85

The half-life of purified GCase85 or enzyme replacement therapy (ERT, velaglucerase alfa) was determined in a range of biologically relevant matrices at a protein concentration of 125 ng/mL in AB (pH 5.6) or PBS, or of 250 ng/mL in mouse serum, mouse plasma, rhesus or cynomolgus plasma, or human serum.

The thermostability of GCase85 was investigated and compared with ERT (velaglucerase alfa) by a thermal shift assay using the QuantStudio 3 and 5 Real-Time PCR systems and SYPRO Orange Protein Gel Stain (Thermo Fisher Scientific, St Louis, MO). Velaglucerase alfa or GCase85, in amounts of 1.5, 3, and 6 μM, were buffer-exchanged (PD-10 desalting columns [VWR]) into neutral (7.0) or lysosomal (5.75) pH and mixed with 5× SYPRO Orange. From a 2-min hold at 25°C, the temperature was increased in increments of 1°C per minute to a final 95°C. The resulting data was used to calculate the melting temperature (resolution of 1°C).

To determine the K_M, purified GCase85 or ERT (velaglucerase alfa) at 3.35 nM was incubated with various concentrations of 4-MUG (0, 0.2, 0.4, 0.6, 0.8, 1, 1.5, 2, 2.5, 3, 4, and 5 mM) in 50 μL AB (pH 5.75) with 1% dimethyl sulfoxide. The reactions were carried out at 37°C, and 4-MU product formation was monitored by measuring fluorescence (excitation at 355 nm and emission at 450 nm) every 1.5 min for ≥26 min of reaction time (beginning 5 min after the start of the reaction).

In silico assessment of GCase-WT and GCase85

The binding affinities of peptides derived from the sequences of human GCase-WT and GCase85 to human leukocyte antigen (HLA) class I and class II receptors (allotypes; Table S5) were used for the *in silico* assessment of the immunogenicity risk. All possible peptide fragments of nine and 15 amino acids were generated *in silico* for calculating predicted binding affinities to HLA I and HLA II receptor molecules, respectively. The fragments were derived from the region spanning 50 amino acids that are N-terminal to the substitution W351C and from the region spanning 50 amino acids that are C-terminal to the substitution A380C. This corresponds to the region starting from residue R301 and ending in P430, with the sequence numbering based on NCBI Reference Sequence: NP_000148.2. The fragment sequences derived from the WT and the GCase variant sequences were used as input for calculations using the tools available in the Immune Epitope Database and Analysis Resource (https://www.iedb.org/). The prediction methods used were NetHLApan EL 4.0 for HLA I and NetHLAIIpan 3.2 for HLA II. The allotypes represent reference sets that are described by Martini S, 2020,[54,55] which provide global population coverages of >97% for HLA I and >99% for HLA II. The calculated half-maximal inhibitory concentration (IC_{50}) values were used as a measure of peptide binding affinity, and IC_{50} cutoff values were used to categorize the peptides as "strong" (IC_{50}, 0 nM to ≤50 nM) or "intermediate" (IC_{50}, >50 nM to ≤500 nM) binders.

Uptake of expressed GCase85 in human cells

Cell lines and preparation

Peripheral blood mononuclear cells (PBMCs, iQB-PBMC103, iQ Biosciences) were seeded at 2×10^5 cells/100 μL/well and maintained in Roswell Park Memorial Institute (RPMI) 1640 medium (Thermo Fisher Scientific, St Louis, MO), supplemented with 10% FBS (Thermo Fisher Scientific, St Louis, MO) and 20 ng/mL of recombinant human macrophage colony stimulating factor (CSF; PeproTech, Rocky Hill, NJ). The PBMCs were incubated for 24 h.

THP-1-derived macrophages (TIB-202, ATCC) were seeded at 3×10^4 cells/100 μL/well and maintained in RPMI 1640 medium, supplemented with 10% FBS and 95.5 ng/mL of phorbol 12-myristate 13-acetate (PMA; Merck, St Louis, MO). THP-1 cells were incubated for 48 h before the medium was changed to RPMI 1640 with 10% FBS (without PMA) and were then incubated for 24 h.

Gaucher disease type 1 (GM00372) and Gaucher disease type 2 (GM01260) human skin-derived fibroblasts (Coriell Institute, New Jersey, USA), were seeded at 2×10^5 cells/100 μL/well in tissue culture-treated flat-bottom 96-well plates (Costar, Corning Life Sciences, St David's Park, UK) and maintained with Dulbecco's Modified Eagle's Medium (high glucose) (Sigma-Aldrich, Dorset, UK) supplemented with 15% FBS (Gibco, Grand Island, NY).

Gaucher disease induced pluripotent stem cell (iPSC) clone A (L444P/L444P) was cultured in feeder-free conditions mTeSR1/mTeSR Plus (STEMCELL Technologies, Cambridge, UK) and differentiated first into monocytes using STEMdiff Monocyte Kit (STEMCELL Technologies, Cambridge, UK) and then into M0 macrophages (unpolarized) using X-VIVO medium supplemented with 100 ng/mL CSF-1, 1× GlutaMAX (Gibco, Grand Island, NY) as per manufacturer protocol. Flow cytometry confirmed that the harvested monocytes were >70% CD14-positive, and the differentiated

macrophages were CD14-, CD206-, CD16-, CD11b-, and CD64-positive from 5 days in CSF-1 (Figure S12).

Treatment with GCase85 or ERT (velaglucerase alfa)

PBMCs and THP-1 cells were treated with five different concentrations (0.1, 0.5, 1, 5, and 50 μg/mL) of purified GCase from FLT201 (AAVS3 vector encoding *GBA1-85*) or ERT (velaglucerase alfa; Takeda Pharmaceuticals) for 3 h, with fresh enzymes being added to the culture media every hour. Gaucher disease patient-derived skin fibroblasts were treated with four different concentrations (0.1, 0.5, 1, and 5 μg/mL) of purified FLT201 (GCase85) or ERT (velaglucerase alfa) for 3 h, with culture media removed (without washing) and replaced every hour with fresh media containing fresh enzymes, and then incubated overnight at 37°C.

GCase uptake in Gaucher disease iPSC-derived macrophages was assessed following a 3-h incubation with cell culture supernatant collected from FLT201-transduced Huh7 cells at different MOI levels (10^4, 10^5, 10^6 vg/cell). In another experiment, Gaucher disease iPSC-derived macrophages were treated with purified GCase from FLT201 or commercial recombinant enzyme at three different concentrations (1.25, 2.5, and 5 μg/mL) in the presence or absence of mannan (2 mg/mL).

Following treatment, the cells (PBMCs, THP-1, Gaucher disease patient-derived skin fibroblasts, or iPSC-derived macrophages) were thoroughly washed three times in cold PBS-1X and treated with 55 μL of fresh lysis buffer (Mammalian Cell PE LB, G-Biosciences, St Louis, MO) supplemented with 0.1% taurocholate (Merck, St Louis, MO), 0.025% Triton X-100, and 1% Halt protease and phosphate inhibitor cocktail (Thermo Fisher Scientific, St Louis, MO) for 10 min at room temperature. The cell lysate was transferred to −80°C prior to GCase activity assay. The GCase activity assay was performed as described earlier (see GCase enzyme activity *in vitro* section above).

Mouse models and treatment

WT mice

Male C57BL/6J mice (Charles River, Little Chesterford, UK), aged ∼7–8 weeks, were used. Mice were dosed intravenously via the lateral tail vein. Procedures were performed at RxCelerate Ltd and the Royal Free Campus of University College London, in accordance with the guidelines of the United Kingdom Animals (Scientific Procedures) Act 1986 Amendment Regulations 2012. Experimental procedures were carried out under Procedures Project License number PAE2D0A13 and PEF024449E. All experimental procedures performed were approved by the ethical review board of the University of Cambridge and the UK Home Office.

GCase-deficient mice

$GBA^{D409V/null}$ (9V/null) mice were generated at Cincinnati Children's Hospital Medical Center (CCHMC) by crossing mice carrying the *Gba1* mutation D409V/D409V (9V/9V) and mice that were *Gba1* null/WT.[56,57] The 9V/null line has a mixed background composed of C57BL/6, 129SvEvBrd, and FVB. Mice from multiple litters were randomly assigned to each treatment group on a rolling basis. Mice, aged 8 weeks with body weights of 20–30 g, were enrolled in each group before overt disease onset (n = 10–16). Due to vector availability, animals were enrolled to the two arms AAV8-*GBA1-WT* or AAV8-*GBA1-85* in two stages, with animals enrolled to the vehicle-treated 9V/null control group at both stages and combined. The animal housing space at CCHMC is accredited by Association for Assessment and Accreditation of Laboratory Animal Care and meets or exceeds the Animal Welfare Act requirement. The CCHMC Institutional Animal Care and Use Committee reviewed and approved these studies under protocol 2018-0056.

AAV8-*GBA1-85* viral stock (2.7×10^{12} vg/mL) and AAV8-*GBA1-WT* viral stock (7.33×10^{12} vg/mL) were diluted with X-VIVO 10 (pH 7.0; Lonza) to 2×10^{10}, 2×10^{11}, or 2×10^{12} vg/mL. Treatment was administered by intravenous tail vein injection (5 μL/g body weight). ERT (velaglucerase alfa) was diluted with acidified X-vivo 10 (pH 5.6, 4°C) to 0.024 U/μL and administered at 60 U/kg, 2.5 μL/g body weight every 2 weeks (seven injections in total). Vehicle (X-VIVO, pH 7.0) at 5 μL/g was also administered. The injections were performed while mice were under anesthesia with isoflurane.

Plasma and tissue collection

WT mice

WT mice had blood collected by cardiac puncture at 28 or 42 days after injection and were euthanized by cervical dislocation. Plasma was obtained from whole blood collected in ethylenediaminetetraacetic acid (EDTA) and centrifuged. Plasma was divided into three equal undiluted aliquots and three aliquots of diluted plasma (∼1:25 AB) to a total volume of 250 μL). All plasma samples were then snap-frozen on dry ice and stored at −80°C until required for analysis of GCase activity. Selected tissues (liver, spleen, lung, and bone marrow) were dissected out and snap-frozen. For immunohistochemical analysis, liver, lung, spleen, and bone marrow were preserved in formalin.

GCase-deficient mice

The 9V/null mice were euthanized using pentobarbital (100 mg/kg) 12 weeks after injection. Blood (∼700 μL) was collected via portal vein into 0.5 M EDTA (20 μL) tubes, with a portion (∼400 μL) processed to collect white blood cells (WBCs). The remaining blood was processed to plasma and stored at −80°C for further analysis or processed for activity assay within 2 h of collection. Mice were transcardially perfused with saline; liver, spleen, and lung were dissected out, with one part fixed in 10% formalin for histology analysis and three parts frozen at −80°C until required for further analysis. In addition, bone marrow cells were collected from femurs and tibias of both legs and stored at −80°C.

WBCs were isolated from the portion of blood reserved for that purpose (∼400 μL). The blood was suspended in 10× volume of PBS and centrifuged to separate the cells. The cells were suspended in

10× volume of red blood cell lysis buffer (8.3 g/L NH_4Cl in 0.01 M tris-HCl buffer, pH 7.5) and centrifuged. The lysis procedure was repeated three times until the pellets were a pale color. The final WBCs were washed with PBS, collected by centrifugation, and stored at −80°C.

GCase enzyme activity in mouse tissues and cells

WT mice

Frozen solid tissue (spleen and lung, 30–50 mg) were transferred to cool in Precellys 2 mL CK-14 homogenizing tubes containing 400 μL of freshly made lysis buffer. Frozen solid tissues were homogenized using a Precellys Evolution Tissue Homogenizer (1 × 20 s, 2,000 × *g*, or 5,500 rpm). Pelleted isolated cells (PBMCs and bone marrow) were already suspended in 200 μL of lysis buffer. Extracts of bone marrow, spleen, and liver samples were lysed by grinding with a conical pellet pestle attached to a cordless drill.

Tissue and cell lysates were incubated at 4°C for 10 min prior to centrifugation to clarify the homogenates (10 min, 4°C, 13,000 × *g*). Tissue protein concentration was determined using the bicinchoninic acid (BCA) protein assay kit following the manufacturer's protocol for a 96-well microplate format (Pierce, Eureka, MO). Protein lysates and bovine serum albumin (BSA) standards were assayed in duplicate. Protein concentrations were extrapolated by reference to a BSA linear seven-point standard curve (125–2,000 μg/mL, including blank). Dilution of plasma and protein lysate samples differed depending on the dose group and tissue type. Samples (25 μL) were incubated with 25 μL of 6 mM 4-MUG for 30 min at 37°C. After incubation, stop solution (50 μL) was added, and enzyme activity was assessed fluorometrically as described for the *in vitro* experiments. GCase-specific activity was estimated based on a seven-point ERT (velaglucerase alfa) standard curve for each sample.

9V/null mice

WBC, bone marrow, and tissue samples were homogenized in 1% sodium taurocholate and 1% Triton X-100, using the Precellys 2 mL tissue-homogenizing mixed-beads kit (Bertin Instruments, Montigny-le-Bretonneux, France) and a Precellys Evolution tissue homogenizer with Cryolys thermo control (4°C, Bertin Instruments, Montigny-le-Bretonneux, France) for two cycles (20 s each, at 30-s interval) at 4°C. Cells (bone marrow and WBCs) were homogenized in sodium taurocholate and 1% Triton X-100 with sonication at 4°C. Tissue and cell lysates (2 μL) were diluted (5×) with reaction buffer in the assay mixture (0.025 M citric phosphate buffer, pH 5.6). Plasma was diluted in 0.025 M citric phosphate buffer (pH 5.6).

GCase activity was determined fluorometrically (Molecular Devices M5 fluorospectrometer) for RFU, following incubation for 1 h at 37°C with 4-MUG (4 mM; Biosynth AG, Staad, Switzerland) in the presence and absence of 2 mM conduritol B epoxide (CBE, Merck Millipore, St Louis, MO), an irreversible GCase inhibitor, to estimate levels of non-acid-β-glucosidase that cleaves 4-MUG. The coefficient factor for 4-MUG is 56,500, derived from a 4-MU standard curve. Protein concentrations in the lysate of tissues and cells were determined using BCA protein assay reagent (Pierce, Eureka, MO). The negative control contained 4-MUG in reaction buffer without samples. For plasma samples, GCase activity was determined fluorometrically with 4-MUG without CBE and assayed as above, normalized by plasma volume.

GCase protein was determined: Frozen tissues (liver, spleen, lung, brain) were weighted and homogenized in radioimmunoprecipitation assay buffer (RIPA) buffer using Precellys 2 mL Tissue Homogenizing Mixed Beads kit and Precellys Evolution tissue homogenizer with Cryolys thermo control (4°C). The program cycle was 20 s twice with 30-s break between two cycles. The homogenized samples were centrifuged (2,000 × *g*, 5 min). The tissue lysates were collected, diluted with the dilution buffer provided in ELISA kit (LSBio, Seattle, WA; LS-6515), and transferred to 96-well plates (4°C). Sample dilution factors were chosen based on their pre-determined GCase activity, e.g., liver (100- to 300-fold), lung (200-fold), spleen (100- to 300-fold), and brain (50-fold). Plasma was diluted 100-fold. ELISA GBA standard curve (STD) was set at a range of 4,000 pg/mL to 31.25 pg/mL. STD was included on each plate. Each plate contained three Vehicle-9V/null samples for background baseline. GCase quantity of each sample was calculated based on the STD on the same plate using PRISM 8 software (PRISM 8.0.1 version).

Immunohistochemistry of GCase expression

WT mice

Spleen, liver, lung, and bone marrow were collected from each group ($n = 5$). Tissue sections were prepared by standard microtomy or cryosectioning and were processed for GCase immunostaining using the automated Ventana Discovery XT system (Roche Diagnostics, St Louis, MO) and the Ventana 3,3′-diaminobenzidine (DAB) Map Detection Kit. Paraffin sections (10 μm thick) were deparaffinized by graded ethanol and xylene washes; heat-mediated EDTA-based antigen retrieval was carried out by immersing the slides in the Ventana CC1 buffer at sub-boiling temperature for 45 min. Tissue sections were stained with anti-GCase antibody (1:100; ab125065, Abcam, Cambridge, UK) for 4 h at ambient temperature, followed by incubation with horseradish-peroxidase-conjugated swine anti-rabbit antibody (Agilent Dako, Santa Clara, CA) for 30 min. Tissue sections were developed using conventional DAB in the presence of hydrogen peroxide and counterstained with hematoxylin to visualize nuclei. Positive staining was visualized by intense brown staining, a result of the oxidation of DAB by hydrogen peroxide. The entire stained section was scanned using an automated digital slide scanner (NanoZoomer S360 digital slide scanner C13220-01, Hamamatsu Photonics). Brightfield representative images of the slides presented in this article were acquired at ×40 magnification.

Lysosomal colocalization of GCase in macrophages

WT mice

Immunostaining with antibodies against mouse LAMP1 and mouse F4/80 was used to assess colocalization of human GCase to lysosomes and macrophages, respectively, in spleen cryosections from WT mice (C57BL/6) treated with AAV8-*GBA1-85*. Spleen

cryosections from five AAV8-*GBA1-85*-treated mice (2×10^{12} vg/kg) were incubated with 1% sodium dodecyl sulfate and permeabilized with 0.25% Triton X-100. Sections were incubated with anti-human GCase (ab125065, Abcam, Cambridge, UK) and either anti-LAMP1 (ab25245, Abcam) or anti-F4/80 (MA191124; Invitrogen, Carlsbad, CA) antibodies. Sections were then incubated with appropriately labeled secondary antibodies and imaged by confocal microscopy. Images were captured for costained sections using the Nikon A1R confocal microscope. Images were captured with a resolution of 2048 × 2048 (pixel size, 0.1032 μm) and processed using Imaris Image Analysis Software (Version 9.2.1, Bitplane).

Liquid chromatography-mass spectrometry of substrate in 9V/null mice

Frozen liver, spleen, and lung (∼50 mg) were homogenized in 3.6 mL of methanol/chloroform/water (2:1:0.6 v/v/v) for 15 s using Omni Tip homogenizing kit with 7 mm stainless steel generator probe (OMNI International, Kennesaw, GA). Bone marrow cells were suspended in 200 μL of water, sonicated, then vortexed to make cell lysate. For liquid chromatography-mass spectrometry (LC-MS) analysis, 500 μL of tissue lysate, ∼100 μL of plasma, and 160 μL of bone marrow cell lysate were used. The substrate (glucosylceramide and glucosylsphingosine) levels were quantitated by LC-MS at the Medical University of South Carolina Lipidomics Shared Resource Analytical Unit. Glucosylceramide and glucosylsphingosine levels were normalized to tissue weight or plasma volume used. For bone marrow, the remaining lysate was used for protein estimation. Glucosylceramide and glucosylsphingosine levels in bone marrow were normalized to the amount of protein.

Hexosylsphingosine includes glucosylsphingosine and galactosylsphingosine and hexosylceramide includes glucosylceramide and galactosylceramide; given that galactosyl-lipids are undetectable in plasma, liver, spleen, lung, and bone marrow, hexosylceramide and hexosylsphingosine were quantified to represent glucosylceramide and glucosylsphingosine, respectively. The lower limit of quantitation was 25 pmol/mL.

Histology analysis of activated macrophages and inflammation in 9V/null mice

Liver and lung were dissected from saline-perfused 9V/null mice, fixed in formalin (10%) and embedded in paraffin; 4-μm sections were mounted on slides.

For the storage cell counts, tissue sections were stained with hematoxylin and eosin using Leica Autostainer XL. The stained tissues were scanned with Aperio AT2 (20×; Leica Biosystems, Deer Park, IL) and processed using Aperio eSlide Image Scope. Storage cells (macrophages >10 μm in liver and >15 μm in lung) were manually counted on randomly selected images (10 for liver and 10 for lung) and averaged. Representative images are presented in Figure S8.

For CD68 staining signal (an inflammatory marker in Gaucher disease), tissue sections were stained with rabbit anti-mouse CD68 antibody (1:25; ab53444; Abcam, Cambridge, UK) using a Discover Ultra immunohistochemistry/*in situ* hybridization slide-staining machine. Tissues were counterstained with hematoxylin (blue) to visualize cell nuclei. Stained tissues were scanned and processed as described for the storage cells. Immunohistochemistry signals from five images of liver or lung per mouse were analyzed for CD68 signal (brown) using Fiji ImageJ. CD68 staining was assessed in two separate experiments. The intensity variation (conversion factor) was applied to calibrate the CD68 staining intensity between the two experiments, determined from a set of reference samples (three male, three female Vehicle-9V/null) from each experiment. Average CD68 signals observed across the five images analyzed per mouse were used for this analysis. Representative images are presented in Figure S9.

GCase activity in FLT201-treated rhesus macaques

The Keeling Center for Comparative Medicine and Research at MD Anderson Cancer Center reviewed and approved nonhuman primate studies under protocol IACUC #00001785 and are compliant with the Code of Federal Regulations, 21 CFR Parts 58 and 11.

Four male and three female rhesus macaques were dosed with FLT201 at 2×10^{12} vg/kg and followed for up to 6 months in three male (age at dosing: two at 3 years 4 months, one at 3 years 3 months) and two female animals (age at dosing: 3 years 4 months) and up to 60 months in one male (age at dosing: 1 year) and one female (age at dosing: 3.5 years) animal. Relative to the other animals on study, animal 7 was lighter (entering the study at 1 year old) and received approximately 50% lower total dose resulting in a lower peak GCase plasma activity and does not reflect a male-female difference in expression. Animal characteristics and total dose infused can be found in Table S4. Plasma GCase activity levels were determined weekly during the first 2 months, monthly for up to 6 months, and every 3 months thereafter (see final paragraph of the GCase enzyme activity in mouse tissues and cells section; incubation with 4-MUG was for 30 min instead of 1 h).

Anti-GCase antibody analysis in FLT201-treated rhesus macaques

ELISA plates (Maxisorp, Nunc, London, UK) were coated with GBA (VPRIV, Shire, Dublin, Ireland) and blocked with BSA (A4503, Sigma-Aldrich, Dorset, UK). Standard curve was generated using serial dilutions of human anti-GBA IgG1 mAb (AbD45646ia, Bio-Rad, Hertfordshire, UK), alongside NHP plasma samples. Plates were incubated with in-house biotinylated (EZ-LinkSulfo-NHS-Biotinylation Kit 21425, Thermo Fisher Scientific, St Louis, MO) GBA (VPRIV, Shire, Dublin, Ireland), followed by Streptavidin-HRP (21130, Thermo Fisher Scientific, St Louis, MO). Signal was developed using TMB (T4444, Sigma-Aldrich, Dorset, UK) and OD measured at 450 nm.

DATA AVAILABILITY

The data and unique biological materials that support the findings of this study are available from the corresponding author (Rose Sheridan) or Spur Therapeutics (medicalinformation@spurtherapeutics.com), upon reasonable request.

ACKNOWLEDGMENTS

This research was funded by Spur Therapeutics Limited.

Alex Dimokov performed anti-GCase antibody analysis. Cindy Zhu and Professor Ian E. Alexander (the Children's Medical Research Institute, Westmead NSW, Australia) performed the *in vivo* FRG mouse experiments. Medical writing assistance and editorial support was provided by Nancy Griffith, PhD, Patrick Flight, PhD, and Katrina Paumier, PhD, of Spur Therapeutics and by Ruth Gandolfo, PhD, and Tamzin Gristwood, PhD, of Oxford PharmaGenesis, Oxford, UK, which was sponsored by Spur Therapeutics in accordance with Good Publication Practice 2022 guidelines.

AUTHOR CONTRIBUTIONS

F.C., C.J.M., R.C., R.S., and A.C.N. conceived the study; Y.S., G.T., J.M.J., F.C., C.J.M., and A.D. designed the experiments; B.L., T.D., M.C., C.C., K.K., E.C., E. Stotter, E. Shehu, S.S., I.-M.Y., J.P., N.N., P.K., A.D., and S.C. performed the experiments; J.M.J., J.K., E. Shehu, I.-M.Y., A.D., and R.S. analyzed the data; F.C., C.J.M., J.M.J., and M.C. wrote the first draft manuscript and prepared the figures; all authors reviewed and edited the manuscript and provided approval of the final submitted version.

DECLARATION OF INTERESTS

F.C., C.J.M., T.D., J.M.J., M.C., C.C., K.K., E.C., E. Stotter, E. Shehu, S.S., I.-M.Y., J.P., J. K., N.N., P.K., S.C., A.D., R.S., and R.C. were or are full-time employees of Spur Therapeutics; A.C.N. was a consultant to Spur Therapeutics. This work has been in part described in one or more pending and granted patent applications.

SUPPLEMENTAL INFORMATION

Supplemental information can be found online at https://doi.org/10.1016/j.ymthe.2025.05.003.

REFERENCES

1. Stirnemann, J., Belmatoug, N., Camou, F., Serratrice, C., Froissart, R., Caillaud, C., Levade, T., Astudillo, L., Serratrice, J., Brassier, A., et al. (2017). A Review of Gaucher Disease Pathophysiology, Clinical Presentation and Treatments. Int. J. Mol. Sci. *18*, 441–471.
2. Nalysnyk, L., Rotella, P., Simeone, J.C., Hamed, A., and Weinreb, N. (2017). Gaucher disease epidemiology and natural history: a comprehensive review of the literature. Hematology *22*, 65–73.
3. Charrow, J., Andersson, H.C., Kaplan, P., Kolodny, E.H., Mistry, P., Pastores, G., Rosenbloom, B.E., Scott, C.R., Wappner, R.S., Weinreb, N.J., and Zimran, A. (2000). The Gaucher registry: demographics and disease characteristics of 1698 patients with Gaucher disease. Arch. Intern. Med. *160*, 2835–2843.
4. Barton, N.W., Brady, R.O., Dambrosia, J.M., Di Bisceglie, A.M., Doppelt, S.H., Hill, S.C., Mankin, H.J., Murray, G.J., Parker, R.I., Argoff, C.E., et al. (1991). Replacement Therapy for Inherited Enzyme Deficiency — Macrophage-Targeted Glucocerebrosidase for Gaucher's Disease. N. Engl. J. Med. *324*, 1464–1470.
5. Gary, S.E., Ryan, E., Steward, A.M., and Sidransky, E. (2018). Recent advances in the diagnosis and management of Gaucher disease. Expert Rev. Endocrinol. Metab. *13*, 107–118.
6. Hughes, D.A., and Pastores, G.M. (2000). [Updated 2023 Dec 7]. Gaucher Disease. In GeneReviews® [Internet], M.P. Adam, J. Feldman, G.M. Mirzaa, R.A. Pagon, S.E. Wallace, and A. Amemiya, eds. (University of Washington, Seattle), pp. 1993–2024.
7. Shawky, R.M., and Elsayed, S.M. (2016). Treatment options for patients with Gaucher disease. Egypt. J. Med. Hum. Genet. *17*, 281–285.
8. Weinreb, N.J., Goldblatt, J., Villalobos, J., Charrow, J., Cole, J.A., Kerstenetzky, M., vom Dahl, S., and Hollak, C. (2013). Long-term clinical outcomes in type 1 Gaucher disease following 10 years of imiglucerase treatment. J. Inherit. Metab. Dis. *36*, 543–553.
9. Weinreb, N.J., Camelo, J.S., Charrow, J., McClain, M.R., Mistry, P., and Belmatoug, N.; International Collaborative Gaucher Group ICGG Gaucher Registry NCT00358943 investigators (2021). Gaucher disease type 1 patients from the ICGG Gaucher Registry sustain initial clinical improvements during twenty years of imiglucerase treatment. Mol. Genet. Metab. *132*, 100–111.
10. Wyatt, K., Henley, W., Anderson, L., Anderson, R., Nikolaou, V., Stein, K., Klinger, L., Hughes, D., Waldek, S., Lachmann, R., et al. (2012). The effectiveness and cost-effectiveness of enzyme and substrate replacement therapies: a longitudinal cohort study of people with lysosomal storage disorders. Health Technol. Assess. *16*, 1–543.
11. Mehta, A. (2008). Gaucher disease: unmet treatment needs. Acta Paediatr. *97*, 83–87.
12. Massaro, G., Geard, A.F., Liu, W., Coombe-Tennant, O., Waddington, S.N., Baruteau, J., Gissen, P., and Rahim, A.A. (2021). Gene Therapy for Lysosomal Storage Disorders: Ongoing Studies and Clinical Development. Biomolecules *11*, 611.
13. Nagree, M.S., Scalia, S., McKillop, W.M., and Medin, J.A. (2019). An update on gene therapy for lysosomal storage disorders. Expert Opin. Biol. Ther. *19*, 655–670.
14. Deegan, P.B., and Cox, T.M. (2012). Imiglucerase in the treatment of Gaucher disease: a history and perspective. Drug Des. Devel. Ther. *6*, 81–106.
15. Tekoah, Y., Tzaban, S., Kizhner, T., Hainrichson, M., Gantman, A., Golembo, M., Aviezer, D., and Shaaltiel, Y. (2013). Glycosylation and functionality of recombinant β-glucocerebrosidase from various production systems. Biosci. Rep. *33*, e00071–e00781.
16. Xu, Y.-H., Sun, Y., Barnes, S., and Grabowski, G.A. (2010). Comparative Therapeutic Effects of Velaglucerase Alfa and Imiglucerase in a Gaucher Disease Mouse Model. PLoS One *5*, e10750.
17. Chowdary, P., Shapiro, S., Makris, M., Evans, G., Boyce, S., Talks, K., Dolan, G., Reiss, U., Phillips, M., Riddell, A., et al. (2022). Phase 1–2 Trial of AAVS3 Gene Therapy in Patients with Hemophilia B. N. Engl. J. Med. *387*, 237–247.
18. Nathwani, A.C., Gray, J.T., Ng, C.Y.C., Zhou, J., Spence, Y., Waddington, S.N., Tuddenham, E.G.D., Kemball-Cook, G., McIntosh, J., Boon-Spijker, M., et al. (2006). Self-complementary adeno-associated virus vectors containing a novel liver-specific human factor IX expression cassette enable highly efficient transduction of murine and nonhuman primate liver. Blood *107*, 2653–2661.
19. Au, H.K.E., Isalan, M., and Mielcarek, M. (2021). Gene Therapy Advances: A Meta-Analysis of AAV Usage in Clinical Settings. Front. Med. *8*, 809118.
20. Miao, C.H., Ohashi, K., Patijn, G.A., Meuse, L., Ye, X., Thompson, A.R., and Kay, M. A. (2000). Inclusion of the Hepatic Locus Control Region, an Intron, and Untranslated Region Increases and Stabilizes Hepatic Factor IX Gene Expression in Vivo but Not in Vitro. Mol. Ther. *1*, 522–532.
21. Dang, Q., Walker, D., Taylor, S., Allan, C., Chin, P., Fan, J., and Taylor, J. (1995). Structure of the Hepatic Control Region of the Human Apolipoprotein E/C-I Gene Locus. J. Biol. Chem. *270*, 22577–22585.
22. Hafenrichter, D.G., Wu, X., Rettinger, S.D., Kennedy, S.C., Flye, M.W., and Ponder, K.P. (1994). Quantitative evaluation of liver-specific promoters from retroviral vectors after *in vivo* transduction of hepatocytes. Blood *84*, 3394–3404.
23. Hughes, D.A., Barton, S., Chan, J., Sherry, N., and Long, A. (2022). Design of GALILEO-1, a phase 1/2 safety and efficacy study of FLT201 in adult patients with Gaucher disease type 1. Mol. Genet. Metab. *135*, S57–S58.
24. Takeda (2024). VPRIV 400 Units Powder for Solution for Infusion - Summary of Product Characteristics (SmPC), pp. 1–9.
25. Wright, P.B., McDonald, E., Bravo-Blas, A., Baer, H.M., Heawood, A., Bain, C.C., Mowat, A.M., Clay, S.L., Robertson, E.V., Morton, F., et al. (2021). The mannose receptor (CD206) identifies a population of colonic macrophages in health and inflammatory bowel disease. Sci. Rep. *11*, 19616.
26. Evren, E., Ringqvist, E., Tripathi, K.P., Sleiers, N., Rives, I.C., Alisjahbana, A., Gao, Y., Sarhan, D., Halle, T., Sorini, C., et al. (2021). Distinct developmental pathways from blood monocytes generate human lung macrophage diversity. Immunity *54*, 259–275.e7.
27. Sun, Y., Liou, B., Chu, Z., Fannin, V., Blackwood, R., Peng, Y., Grabowski, G.A., Davis, H.W., and Qi, X. (2020). Systemic enzyme delivery by blood-brain barrier-penetrating SapC-DOPS nanovesicles for treatment of neuronopathic Gaucher disease. EBioMedicine *55*, 102735.
28. Kallemeijn, W.W., Scheij, S., Hoogendoorn, S., Witte, M.D., Herrera Moro Chao, D., van Roomen, C.P.A.A., Ottenhoff, R., Overkleeft, H.S., Boot, R.G., and Aerts, J.M.F. G. (2017). Investigations on therapeutic glucocerebrosidases through paired detection with fluorescent activity-based probes. PLoS One *12*, e0170268.

29. Hughes, D.A., Canaan-Kühl, S., Barton, S., Collis, R., and Sherry, N. (2022). Safety and efficacy of FLT190 for the treatment of patients with Fabry disease: Results from the MARVEL-1 Phase 1/2 clinical trial Paper Presented at the 18th Annual WORLD Symposium; (Elsevier Inc).

30. He, T., Itano, M.S., Earley, L.F., Hall, N.E., Riddick, N., Samulski, R.J., and Li, C. (2019). The Influence of Murine Genetic Background in Adeno-Associated Virus Transduction of the Mouse Brain. Hum. Gene Ther. Clin. Dev. *30*, 169–181.

31. Fallet, S., Grace, M.E., Sibille, A., Mendelson, D.S., Shapiro, R.S., Hermann, G., and Grabowski, G.A. (1992). Enzyme Augmentation in Moderate to Life-Threatening Gaucher Disease. Pediatr. Res. *31*, 496–502.

32. Bove, K.E., Daugherty, C., and Grabowski, G.A. (1995). Pathological findings in gaucher disease type 2 patients following enzyme therapy*1. Hum. Pathol. *26*, 1040–1045.

33. Beutler, E. (2004). Enzyme Replacement in Gaucher Disease. Plos Med. *1*, e21.

34. Figueroa, M.L., Rosenbloom, B.E., Kay, A.C., Garver, P., Thurston, D.W., Koziol, J. A., Gelbart, T., and Beutler, E. (1992). A Less Costly Regimen of Alglucerase to Treat Gaucher's Disease. N. Engl. J. Med. *327*, 1632–1636.

35. Beutler, E., Kay, A., Saven, A., Garver, P., Thurston, D., Dawson, A., and Rosenbloom, B. (1991). Enzyme replacement therapy for Gaucher disease. Blood *78*, 1183–1189.

36. Simonaro, C.M. (2016). Lysosomes, Lysosomal Storage Diseases, and Inflammation. J. Inborn Errors Metab. Screen. *4*, 232640981665046.

37. Abeliovich, A., Hefti, F., and Sevigny, J. (2021). Gene Therapy for Parkinson's Disease Associated with GBA1 Mutations. J. Parkinsons Dis. *11*, S183–S188.

38. Neuhaus, S., Weaver, M., Goker-Alpan, O., Cohen, J.L., Giraldo, P., Booth, J., Shaughnessy, L., Hatch, D., Uspenskaya, O., and Sevigny, J. (2025). Phase 1/2 dose-finding study to evaluate systemic administration of an AAV9-based gene therapy for peripheral manifestation of Gaucher disease: The PROCEED study. Mol. Genet. Metab. *144*, 108873.

39. Enquist, I.B., Nilsson, E., Ooka, A., Månsson, J.-E., Olsson, K., Ehinger, M., Brady, R. O., Richter, J., and Karlsson, S. (2006). Effective cell and gene therapy in a murine model of Gaucher disease. Proc. Natl. Acad. Sci. USA *103*, 13819–13824.

40. Dahl, M., Smith, E.M.K., Warsi, S., Rothe, M., Ferraz, M.J., Aerts, J.M.F.G., Golipour, A., Harper, C., Pfeifer, R., Pizzurro, D., et al. (2021). Correction of pathology in mice displaying Gaucher disease type 1 by a clinically-applicable lentiviral vector. Mol. Ther. Methods Clin. Dev. *20*, 312–323.

41. Heckman, L.D., Sheehan, P., Fenn, T., Wong, L.C., Nelson, S., Garimalla, S., Haller, J., Daily, J., Politi, J., Dai, Y., et al. (2020). Gene therapy PR001 increased GCase activity and improved neuronopathic Gaucher disease phenotypes in mouse models. Mol. Genet. Metab. *129*, S70–S71.

42. Jeyakumar, J.M., Kia, A., Tam, L.C.S., McIntosh, J., Spiewak, J., Mills, K., Heywood, W., Chisari, E., Castaldo, N., Verhoef, D., et al. (2023). Preclinical evaluation of FLT190, a liver-directed AAV gene therapy for Fabry disease. Gene Ther. *30*, 487–502.

43. Nietupski, J.B., Hurlbut, G.D., Ziegler, R.J., Chu, Q., Hodges, B.L., Ashe, K.M., Bree, M., Cheng, S.H., Gregory, R.J., Marshall, J., and Scheule, R.K. (2011). Systemic Administration of AAV8-a-galactosidase A Induces Humoral Tolerance in Nonhuman Primates Despite Low Hepatic Expression. Mol. Ther. *19*, 1999–2011.

44. Hurlbut, G.D., Ziegler, R.J., Nietupski, J.B., Foley, J.W., Woodworth, L.A., Meyers, E., Bercury, S.D., Pande, N.N., Souza, D.W., Bree, M.P., et al. (2010). Preexisting Immunity and Low Expression in Primates Highlight Translational Challenges for Liver-directed AAV8-mediated Gene Therapy. Mol. Ther. *18*, 1983–1994.

45. Pastores, G.M., Turkia, H.B., Gonzalez, D.E., Ida, H., Tantawy, A.A.G., Qin, Y., Qiu, Y., Dinh, Q., and Zimran, A. (2016). Development of anti-velaglucerase alfa antibodies in clinical trial-treated patients with Gaucher disease. Blood Cells Mol. Dis. *59*, 37–43.

46. Mingozzi, F., Liu, Y.-L., Dobrzynski, E., Kaufhold, A., Liu, J.H., Wang, Y., Arruda, V. R., High, K.A., and Herzog, R.W. (2003). Induction of immune tolerance to coagulation factor IX antigen by *in vivo* hepatic gene transfer. J. Clin. Invest. *111*, 1347–1356.

47. Cao, O., Dobrzynski, E., Wang, L., Nayak, S., Mingle, B., Terhorst, C., and Herzog, R. W. (2007). Induction and role of regulatory CD4+CD25+ T cells in tolerance to the transgene product following hepatic *in vivo* gene transfer. Blood *110*, 1132–1140.

48. Mingozzi, F., Hasbrouck, N.C., Basner-Tschakarjan, E., Edmonson, S.A., Hui, D.J., Sabatino, D.E., Zhou, S., Wright, J.F., Jiang, H., Pierce, G.F., et al. (2007). Modulation of tolerance to the transgene product in a nonhuman primate model of AAV-mediated gene transfer to liver. Blood *110*, 2334–2341.

49. Burdo, T.H., Chen, C., Kaminski, R., Sariyer, I.K., Mancuso, P., Donadoni, M., Smith, M.D., Sariyer, R., Caocci, M., Liao, S., et al. (2024). Preclinical safety and biodistribution of CRISPR targeting SIV in non-human primates. Gene Ther. *31*, 224–233.

50. Sharma, R., Goker-Alpan, O., Schwartz, I.V.D., Giraldo, P., Whittaker, A., and Ferrante, F. (2025). Results from GALILEO1, a first in human clinical trial of FLT201 AAV-gene therapy in adult patients with Gaucher disease type 1. Mol. Genet. Metab. *144*, 108945.

51. Puigbò, P., Guzmán, E., Romeu, A., and Garcia-Vallvé, S. (2007). OPTIMIZER: a web server for optimizing the codon usage of DNA sequences. Nucleic Acids Res. Suppl. *35*, W126–W131.

52. Schulze, A., Spada, N., Kober, R., Kochmann, E., Lange, S., Prieler, B., Kia, A., Dane, A.P., Nathwani, A.C., Sonntag, F., et al. (2019). Improved Two-Plasmid Packaging System for Manufacturing of AAV Vectors with High Quality and Consistency. Mol. Ther. *27*, 334.

53. Carli, C.D., Boscher, M., Hanselka, S., Jankiewicz, M., Zach, C., Sonntag, F., Schulze, A., Prieler, B., Rehberger, B., Bhatia, J., et al. (2019). A Robust Commercial rAAV-Vector Platform Process Using the iCELLis® 500 Fixed-Bed Bioreactor. Mol. Ther. *27*, 698.

54. Vita, R., Mahajan, S., Overton, J.A., Dhanda, S.K., Martini, S., Cantrell, J.R., Wheeler, D.K., Sette, A., and Peters, B. (2019). The Immune Epitope Database (IEDB): 2018 update. Nucleic Acids Res *47*, D339–D343. https://doi.org/10.1093/nar/gky1006.

55. Martini, S. (2020). HLA allele frequencies and reference sets with maximal population. https://help.iedb.org/hc/en-us/articles/114094151851.

56. Xu, Y.-H., Quinn, B., Witte, D., and Grabowski, G.A. (2003). Viable Mouse Models of Acid β-Glucosidase Deficiency. Am. J. Pathol. *163*, 2093–2101.

57. Polinski, N.K., Martinez, T.N., Gorodinsky, A., Gareus, R., Sasner, M., Herberth, M., Switzer, R., Ahmad, S.O., Cosden, M., Kandebo, M., et al. (2021). Decreased glucocerebrosidase activity and substrate accumulation of glycosphingolipids in a novel GBA1 D409V knock-in mouse model. PLoS One *16*, e0252325.